

# Fluvial carbon dioxide emission from the Lena River basin during spring flood

Sergey N. Vorobyev<sup>1</sup>, Jan Karlsson<sup>2</sup>, Yuri Y. Kolesnichenko<sup>1</sup>, Mikhail A. Korets<sup>3</sup>,  
and Oleg S. Pokrovsky<sup>4,5\*</sup>

<sup>1</sup>*BIO-GEO-CLIM Laboratory, Tomsk State University, Tomsk, Russia*

<sup>2</sup>*Climate Impacts Research Centre (CIRC), Department of Ecology and Environmental Science, Umeå University, Linnaeus väg 6, 901 87 Umeå, Sweden.*

<sup>3</sup>*V.N. Sukachev Institute of Forest of the Siberian Branch of Russian Academy of Sciences – separated department of the KSC SB RAS, Krasnoyarsk, 660036, Russia*

<sup>4</sup>*Geosciences and Environment Toulouse, UMR 5563 CNRS, 14 Avenue Edouard Belin 31400 Toulouse, France*

<sup>5</sup>*N. Laverov Federal Center for Integrated Arctic Research, Russian Academy of Sciences, Arkhangelsk, Russia*

Key words: CO<sub>2</sub>, C, emission, permafrost, river, export, landscape, Siberia

\* email: oleg.pokrovsky@get.omp.eu

## Abstract

Greenhouse gas (GHG) emission from inland waters of permafrost-affected regions is one of the key factors of circumpolar aquatic ecosystem response to climate warming and permafrost thaw. Riverine systems of central and eastern Siberia contribute a significant part of the water and carbon (C) export to the Arctic Ocean, yet their C exchange with the atmosphere remain poorly known due to lack of *in-situ* GHG concentration and emission estimates. Here we present the results of continuous *in-situ* pCO<sub>2</sub> measurements over a 2600-km transect of the Lena River main stem and lower reaches of 20 major tributaries (together representing watershed area of 1,661,000 km<sup>2</sup>, 66% of the Lena's basin), conducted at the peak of the spring flood. The pCO<sub>2</sub> in Lena (range 400-1400 μatm) and tributaries (range 400-1600 μatm) remained generally stable (within ca. 20 %) over the night/day period and across the river channels.

32 The pCO<sub>2</sub> in tributaries increased northward with mean annual temperature decrease and permafrost  
33 increase; this change was positively correlated with C stock in soil, the proportion of deciduous needle-  
34 leaf forest and the riparian vegetation. Based on gas transfer coefficients obtained from rivers of the  
35 Siberian permafrost zone, we calculated CO<sub>2</sub> emission for the main stem and tributaries. Typical fluxes  
36 ranged from 1 to 2 g C m<sup>-2</sup> d<sup>-1</sup> (>99% CO<sub>2</sub>, < 1 % CH<sub>4</sub>) which is comparable with CO<sub>2</sub> emission measured  
37 in Kolyma, Yukon and Mackenzie and permafrost-affected rivers in western Siberia. The areal C  
38 emissions from lotic waters of the Lena watershed were quantified via taking into account the total area  
39 of permanent and seasonal water of the Lena basin (28,000 km<sup>2</sup>). Assuming 6 months of the year to be  
40 open water period with no emission under ice, the annual C emission from the whole Lena basin is  
41 estimated as 8.3 ± 2.5 Tg C y<sup>-1</sup> which is comparable to the DOC and DIC lateral export to the Arctic  
42 Ocean.

43

44

## 45 **Introduction**

46 Climate warming in high latitudes is anticipated to result in mobilization, decomposition and  
47 atmospheric release of significant amounts of carbon (C) stored in permafrost soils, providing a positive  
48 feedback (Schuur et al. 2015). Permafrost thawing is expected to also increase the lateral C export to  
49 rivers and lakes (Frey and Smith, 2005). The exported permafrost C is relatively labile and largely  
50 degraded to greenhouse gases (GHG) in recipient freshwaters (e.g. Vonk et al., 2015). As a result,  
51 assessment of GHG emission in rivers of permafrost affected regions is crucially important for  
52 understanding the high latitude C cycle under various climate change scenarios (Chadburn et al., 2017;  
53 Vonk et al., 2019). Among six great Arctic rivers, Lena is most emblematic one, situated chiefly within  
54 the continuous permafrost zone and exhibiting the highest seasonal variation in discharge. Over the past  
55 two decades, there has been an explosive interest to the Lena River hydrology (Yang et al., 2002;  
56 Berezovskaya et al., 2005; Smith and Pavelsky, 2008; Ye et al., 2009; Gelfan et al., 2017; Suzuki et al.,  
57 2018), organic C (OC) transport (Lara et al., 1998; Raymond et al., 2007; Semiletov et al., 2011;  
58 Goncalves-Araujo et al., 2015; Kutscher et al., 2017; Griffin et al., 2018) and general hydrochemistry

59 (Gordeev and Sidorov, 1993; Cauwet and Sidorov, 1996; Huh et al., 1998a,b; Huh and Edmond, 1999;  
60 Wu and Huh, 2007; Kuzmin et al., 2009; Pipko et al., 2010; Georgiadi et al., 2019; Juhls et al., 2020)  
61 including novel isotopic approaches for nutrients (Si, Sun et al., 2018) and trace metals such as Li  
62 (Murphy et al., 2019) and Fe (Hirst et al., 2020). This interest is naturally linked to the Lena River  
63 location within the forested continuous permafrost/taiga zone covered by organic-rich yedoma soil.  
64 Under on-going climate warming, the soils of the Lena River watershed are subjected to strong thawing  
65 and active (seasonally unfrozen) layer deepening (Zhang et al., 2005) accompanied by overall increase  
66 in river water discharge (McClelland et al., 2004; Ahmed et al., 2020), flood intensity and frequency  
67 (Gautier et al., 2018). The Lena River exhibits the highest DOC concentration among all great Arctic  
68 rivers (i.e., Holmes et al., 2013) which may reflect weak DOC degradation in the water column and  
69 massive mobilization of both contemporary and ancient OC to the river from the watershed (Feng et al.,  
70 2013; Wild et al., 2019). In contrast to rather limited works on CO<sub>2</sub> and CH<sub>4</sub> emissions from water  
71 surfaces of Eastern Siberia (Semiletov, 1999; Denfeld et al., 2013), extensive studies were performed on  
72 land, in the polygonal tundra of the Lena River Delta (Wille et al., 2008; Bussman, 2013; Sachs et al.,  
73 2008; Kutzbach et al., 2007) and the Indigirka Lowland (van der Molen et al., 2007). Finally, there have  
74 been several studies of sediment and particular matter transport by the Lena River to the Laptev Sea  
75 (Rachold et al., 1996; Dudarev et al., 2006) together with detailed research of the Lena River Delta  
76 (Zubrzycki et al., 2013; Siewert et al., 2016).

77 Surprisingly, despite such extensive research on C transport, storage, and emission in Eastern  
78 Siberian landscapes, C emissions of the Lena River main stem and tributaries remain virtually unknown,  
79 compared to a relatively good understanding of those in the Yukon (Striegl et al., 2012; Stackpoole et  
80 al., 2017), Mackenzie (Horan et al., 2019), Ob (Karlsson et al., 2021; Pipko et al., 2019) and Kolyma  
81 (Denfeld et al., 2013). The only available estimates of C emission from inland waters of the Lena basin  
82 are based on few indirect (calculated gas concentration and modelled fluxes) snapshot data with very low  
83 spatial and temporal resolution (Raymond et al., 2013). Similar to other regions, this introduces  
84 uncertainties and cannot adequately capture total regional C emissions (Abril et al., 2015; Denfeld et al.,  
85 2018; Park et al., 2018; Klaus et al., 2019; Klaus and Vachon, 2020; Karlsson et al., 2021). In particular,

86 no detailed studies at the peak of spring flood have been performed and the information on various  
87 contrasting tributaries of the Lena River remains very limited. As a result, reliable estimations of  
88 magnitude and controlling factors of C emission in the Lena River basin are poorly understood. The  
89 present work represents a first assessment of CO<sub>2</sub> and CH<sub>4</sub> concentration and fluxes of the main stem  
90 and tributaries during the peak of spring flow, via calculating C emission and relating these data to river  
91 hydrochemistry and GIS-based landscape parameters. This should allow identifying environmental  
92 factors controlling GHG concentration and emission in the Lena River watershed in order to use this  
93 knowledge to foresee future changes in C balance of the largest permafrost-affected Arctic river.

94

## 95 **2. Study Site, Materials and Methods**

### 96 *2.1. Lena River and its tributaries*

97 The sampled Lena River main stem and 20 tributaries are located along a 2600 km latitudinal  
98 transect SW to NE and include watersheds of distinct sizes, geomorphology, permafrost extent, lithology,  
99 climate and vegetation (**Fig. 1, S1 A; Table S1**). The total watershed area of the rivers sampled in this  
100 work is approximately 1.66 million km<sup>2</sup>, representing 66% of the entire Lena River basin. Permafrost is  
101 mostly continuous except some patches of discontinuous and sporadic in the southern part of the Lena  
102 basin (Brown et al., 2002). The mean annual air temperatures (MAAT) along the transect ranges from -  
103 5 °C in the southern part of the Lena basin to -9 °C in the central part of the basin. The range of MAAT  
104 for 20 tributaries is from -4.7 to -15.9 °C. The mean annual precipitation ranges from 350-500 mm y<sup>-1</sup> in  
105 the southern and south-western part of the basin to 200-250 mm y<sup>-1</sup> in the central and northern parts  
106 (Chevychelov and Bosikov, 2010). The lithology of the Siberian platform which is drained by the Lena  
107 River is highly diverse and includes Archean and Proterozoic crystalline and metamorphic rocks, Upper  
108 Proterozoic, Cambrian and Ordovician dolostones and limestones, volcanic rocks of Permo-Triassic age  
109 and essentially terrigenous silicate sedimentary rocks of the Phanerozoic. Further description of the Lena  
110 River basin landscapes, vegetation and lithology can be found elsewhere (Rachold et al., 1996; Huh et  
111 al., 1999a, b; Pipko et al., 2010; Semiletov et al., 2011; Kutscher et al., 2017; Juhls et al., 2020).

112 The peak of annual discharge depends on the latitude (**Fig. 1**) and occurs in May in the south  
113 (Ust-Kut) and in June in the middle and low reaches of the Lena River (Yakutsk, Kysyr). From May 29  
114 to June 17, 2016, we moved downstream the Lena River by boat with an average speed of 30 km h<sup>-1</sup>  
115 (Gureyev, 2016). As such, we followed the progression of the spring and moved from the southwest to  
116 the northeast, thus collecting river water at approximately the same stage of maximal discharge. Note  
117 that transect sampling is a common way to assess river water chemistry in extreme environments (Huh  
118 and Edmond, 1999; Spence and Telmer, 2005), and generally, a single sampling during high flow season  
119 provides the best agreement with time-series estimates (Qin et al., 2006). Regular stops each 80-100 km  
120 along the Lena River allowed sampling for major hydrochemical parameters and CH<sub>4</sub> along the main  
121 stem. We also moved 500-1500 m upstream of selected tributaries to record CO<sub>2</sub> concentrations for at  
122 least 1 h and to sample for river hydrochemistry; see examples of spatial coverage in **Fig. S1 B**. From  
123 late afternoon/evening to the next morning, we stopped for sleep but continued to record pCO<sub>2</sub> in the  
124 Lena River main stem (15 sites, evenly distributed over the full 2600 km transect) and two tributaries  
125 (Aldan and Tuolba).

126

## 127 2.2. CO<sub>2</sub> and CH<sub>4</sub> concentrations

128 Surface water CO<sub>2</sub> concentration was measured continuously, *in-situ* by deploying a portable  
129 infrared gas analyzer (IRGA, GMT222 CARBOCAP® probe, Vaisala®; accuracy ± 1.5%) of two ranges  
130 (2 000 and 10 000 ppm). This system was mounted on a small boat in a perforated steel pipe ~0.5 m  
131 below water surface. The tube had two necessary opening of different diameter, which allowed free water  
132 flow with a constant rate during the moving of the boat. The probe was enclosed within a waterproof and  
133 gas-permeable membrane. The key to aqueous deployment of the IRGA sensor is the use of a protective  
134 expanded polytetrafluoroethylene (PTFE) tube or sleeve that is highly permeable to CO<sub>2</sub> but  
135 impermeable to water (Johnson et al., 2009). The material is available for purchase as a flexible tube that  
136 fits over the IRGA sensor (Product number 200-07; International Polymer Engineering, Tempe, Arizona,  
137 USA). We also used a copper mesh screen to minimize biofouling effects (i.e., Yoon et al., 2016).  
138 However these effects are expected to be low in cold waters of the virtually pristine Lena River and its

139 tributaries. During sampling, the sensor was left to equilibrate in the water for 10 minutes before  
140 measurements were recorded.

141 The probe was enclosed and placed into a tube which was submerged 0.5 m below the water  
142 surface. Within this tube, we designed a special chamber that allowed low-turbulent water flow around  
143 the probe without gas bubbles. Previous studies (Park et al., 2021; Crawford et al. 2015; Yoon et al.,  
144 2016) reported some effects of boat speed on sensor CO<sub>2</sub> measurements due to turbulences. Although  
145 the turbulences were minimized in the tube/chamber design used in the present study, on a selected river  
146 transect (~10 km) we have also tested the impact of the boat speed (5, 10, 20, 30 and 40 km h<sup>-1</sup>) on the  
147 sensor performance and have not detected any sizable (> 10%, p < 0.05, n = 25) difference in the CO<sub>2</sub>  
148 concentrations recorded by our system.

149 A Campbell logger was connected to the system allowing continuous recording of the CO<sub>2</sub>  
150 concentration (ppm), water temperature (°C) and pressure (mbar) every minute during 5 minutes over 10  
151 minute intervals yielding 4,285 individual pCO<sub>2</sub>, water temperature and pressure measurements in total.  
152 These data were averaged for 3 consecutive slots of 5 min measurements, which represented the  
153 approximate 20-km interval of the main stem route. CO<sub>2</sub> concentrations in the Lena River tributaries  
154 were measured over the first 500-2000 m distance upstream of the tributary mouth, and comprised  
155 between 5 and 34 measurements for day-time visits and between 305 and 323 individual pCO<sub>2</sub> readings  
156 for each tributary for day-time and night-time monitoring.

157 Sensor preparation was conducted in the lab following the method described by Johnson et al.  
158 (2009). The measurement unit (MI70, Vaisala®; accuracy ± 0.2%) was connected to the sensor allowing  
159 instantaneous readings of pCO<sub>2</sub>. The sensors were calibrated in the lab against standard gas mixtures (0,  
160 800, 3 000, 8 000 ppm; linear regression with R<sup>2</sup> > 0.99) before and after the field campaign. The sensors'  
161 drift was 0.03-0.06% per day and overall error was 4-8% (relative standard deviation, RSD). Following  
162 calibration, post-measurement correction of the sensor output induced by changes in water temperature  
163 and barometric pressure was done by applying empirically derived coefficients following Johnson et al.  
164 (2009). These corrections never exceeded 5% of the measured values. Furthermore, we tested two  
165 different sensors in several sites of the river transect: a main probe used for continuous measurements

166 and another probe used as a control and never employed for continuous measurements. We did not find  
167 any sizable (>10%) difference in measured CO<sub>2</sub> concentration between these two probes.

168 For CH<sub>4</sub> analyses, unfiltered water was sampled in 60-mL Serum bottles and closed without air  
169 bubbles using vinyl stoppers and aluminum caps and immediately poisoned by adding 0.2 mL of  
170 saturated HgCl<sub>2</sub> via a two-way needle system. In the laboratory, a headspace was created by displacing  
171 approx. 40% of water with N<sub>2</sub> (99.999%). Two 0.5-mL replicates of the equilibrated headspace were  
172 analyzed for their concentrations of CH<sub>4</sub>, using a Bruker GC-456 gas chromatograph (GC) equipped with  
173 flame ionization and thermal conductivity detectors. After every 10 samples, a calibration of the detectors  
174 was performed using Air Liquid gas standards (i.e. 145 ppmv). Duplicate injection of the samples showed  
175 that results were reproducible within ±5%. The specific gas solubility for CH<sub>4</sub> (Yamamoto et al., 1976)  
176 was used in calculation of total CH<sub>4</sub> content in the vials and then recalculated to μmol L<sup>-1</sup> of the initial  
177 waters.

178

### 179 *2.3. Chemical analyses of the river water*

180 The dissolved oxygen (CelloX 325; accuracy of ±5%), specific conductivity (TetraCon 325;  
181 ±1.5%), and water temperature (±0.2 °C) were measured in-situ at 20 cm depth using a WTW 3320  
182 Multimeter. The pH was measured using portable Hanna instrument via combined Schott glass electrode  
183 calibrated with NIST buffer solutions (4.01, 6.86 and 9.18 at 25°C), with an uncertainty of 0.01 pH units.  
184 The temperature of buffer solutions was within ± 5°C of that of the river water. The water was sampled  
185 in pre-cleaned polypropylene bottle from 20-30 cm depth in the middle of the river and immediately  
186 filtered through disposable single-use sterile Sartorius filter units (0.45 μm pore size). The first 50 mL of  
187 filtrate was discarded. The DOC and Dissolved Inorganic Carbon (DIC) were determined by a Shimadzu  
188 TOC-VSCN Analyzer (Kyoto, Japan) with an uncertainty of 3% and a detection limit of 0.1 mg/L. Blanks  
189 of MilliQ water passed through the filters demonstrated negligible release of DOC from the filter  
190 material.

191

192

193 2.4. Flux calculation

194 CO<sub>2</sub> flux ( $F_{CO_2}$ ) was calculated following Cai and Wang (1998):

195 
$$F_{CO_2} = K_h k_{CO_2} (C_{water} - C_{air}), \quad (1)$$

196 where  $K_h$  is the Henry's constant corrected for temperature and pressure ( $\text{mol L}^{-1} \text{atm}^{-1}$ ),  $k_{CO_2}$  is the gas  
197 exchange velocity at a given temperature,  $C_{water}$  is the water CO<sub>2</sub> concentration, and  $C_{air}$  is the CO<sub>2</sub>  
198 concentration in the ambient air. We used the average CO<sub>2</sub> concentrations of 402 ppm in May-June 2016  
199 (from 129 stations all over the world, <https://community.wmo.int/wmo-greenhouse-gas-bulletins>), which  
200 is consistent with the value recorded at the nearest Tiksi station in 2016 ( $404 \pm 0.9$  ppm, Ivakhov et al.,  
201 2019). Temperature-specific solubility coefficients were used to calculate respective CO<sub>2</sub> concentrations  
202 in the water following Wanninkhof et al. (1992). To standardize  $k_{CO_2}$  to a Schmidt number of 600, we  
203 used the following equation (Alin et al., 2011; Vachon et al., 2010):

204 
$$k_{600} = k_{CO_2} \left( \frac{600}{Sc_{CO_2}} \right)^{-n} \quad (2)$$

205 where  $Sc_{CO_2}$  is CO<sub>2</sub> Schmidt number for a given temperature ( $t$ , °C) in the freshwater (Wanninkhof, 1992):

206 
$$Sc_{CO_2} = 1911.1 - 118.11t + 3.4527t^2 - 0.041320t^3 \quad (3)$$

207 The exponent  $n$  (Eqn. 2) is a coefficient that describes water surface ( $2/3$  for a smooth water surface  
208 regime while  $1/2$  for a rippled and a turbulent one), and the Schmidt number for 20°C in freshwater is  
209 600. We used  $n = 2/3$  because all water surfaces of sampled rivers were considered flat and had a laminar  
210 flow (Alin et al., 2011; Jähne et al., 1987) with wind speed always below  $3.7 \text{ m s}^{-1}$  (Guérin et al., 2007).

211 In this study, we used a  $k_{CO_2}$  (a median gas transfer coefficient) value of  $4.464 \text{ m d}^{-1}$  measured in  
212 the 4 largest rivers of Western Siberia Lowland (WSL) in June 2015 (Ob', Pur, Pyakupur and Taz rivers,  
213 Karlsson et al., 2021). These rivers are similar to Lena and its tributaries in size, but exhibit lower velocity  
214 than those of the Lena River. In fact, due to more mountainous relief, the Lena River main stem and  
215 tributaries present much higher turbulence than that of the Ob River and tributaries and as such the value  
216  $k_{CO_2}$  used in this study can be considered rather conservative. This value is consistent with the  $k_{CO_2}$   
217 reported for the Kolyma River and its large tributaries ( $k = 3.9 \pm 2.5 \text{ m d}^{-1}$ , Denfeld et al., 2013),

218 tributaries and main stem of the Yukon river basin ( $k_{600} = 4.9 - 7.6 \text{ m d}^{-1}$ , Striegl et al. 2012), large rivers  
219 in the Amazon and Mekong basins ( $k_{600} = 3.5 \pm 2.1 \text{ m d}^{-1}$ , Alin et al., 2011) and with modelling results  
220 of  $k$  for large rivers across the world ( $k = 3 - 4 \text{ m d}^{-1}$ , Raymond et al., 2013). Note that decreasing the  $k$   
221 to most conservative value of  $3 \text{ m d}^{-1}$  of Raymond et al. (2013) will decrease specific emissions by ca.  
222 30 %.

223 Instantaneous diffusive  $\text{CH}_4$  fluxes were calculated using an equation similar to 1 with  $k$  from  
224 western Siberia rivers (Serikova et al., 2018), concentrations of dissolved  $\text{CH}_4$  in the water and air–water  
225 equilibrium  $\text{pCH}_4$  concentration of 1.8 ppm, and mean annual  $\text{pCH}_4$  concentration in the air for 2016  
226 (Mauna Loa Observatory [ftp://aftp.cmdl.noaa.gov/products/trends/ch4/ch4\\_annmean\\_gl.txt](http://aftp.cmdl.noaa.gov/products/trends/ch4/ch4_annmean_gl.txt)) following  
227 standard procedures (Serikova et al., 2018, 2019).

228

#### 229 *2.5. Landscape parameters and water surface area of the Lena basin*

230 The physio-geographical characteristics of the 20 Lena tributaries sampled in this study and the  
231 two points of the Lena main stem (upstream and downstream r. Aldan, **Table S1**) were determined by  
232 applying available digital elevation model (DEM GMTED2010), soil, vegetation, lithological, and  
233 geocryological maps. The landscape parameters were typified using TerraNorte Database of Land Cover  
234 of Russia (Bartalev et al., 2020, <http://terranorte.iki.rssi.ru>). This included various type of forest  
235 (evergreen, deciduous, needleleaf/broadleaf), grassland, tundra, wetlands, water bodies and other area.  
236 The climate and permafrost parameters of the watershed were obtained from CRU grids data (1950-2016)  
237 (Harris et al., 2014) and NCSCD data ([doi:10.5879/ecds/00000001](https://doi.org/10.5879/ecds/00000001), Hugelius et al., 2013), respectively,  
238 whereas the biomass and soil OC content were obtained from BIOMASAR2 (Santoro et al., 2010) and  
239 NCSCD databases. The lithology layer was taken from GIS version of Geological map of the Russian  
240 Federation (scale 1 : 5 000 000, <http://www.geolkarta.ru/>). To test the effect of carbonate rocks on  
241 dissolved C parameters, we distinguished acidic crystalline, terrigenous silicate rocks and dolostones and  
242 limestones of upper Proterozoic, Cambrian and Ordovician age. We quantified river water surface area  
243 using the global SDG database with  $30 \text{ m}^2$  resolution (Pekel et al., 2016) including both seasonal and  
244 permanent water for the open water period of 2016 and for the multiannual average (reference period

245 2000-2004). We also used a more recent GRWL Mask Database which incorporates first order wetted  
246 streams (Allen and Pavelsky, 2018).

247 The Pearson rank order correlation coefficient ( $R_s$ ,  $p < 0.05$ ) was used to determine the  
248 relationship between  $\text{CO}_2$  concentrations and climatic and landscape parameters of the Lena River  
249 tributaries. Further statistical treatment of  $\text{CO}_2$ , DIC and DOC concentration drivers in river waters  
250 included a Principal Component Analysis which allowed to test the effect of various hydrochemical and  
251 climatic parameters on dissolved C pattern. For the PCA treatment, all variables were normalized as  
252 necessary in the standard package of STATISTICA-7 (<http://www.statsoft.com>) because the units of  
253 measurement for various components were different. The factors were identified via the Raw Data  
254 method. To run the scree test, we plotted the eigen values in descending order of their magnitude against  
255 their factor numbers. There was significant decrease in the PCA values between F1 and F2 suggesting  
256 that a maximum of two factors were interpretable.

257

### 258 **3. Results**

#### 259 *3.1. $\text{CO}_2$ , $\text{CH}_4$ , DIC and DOC in the main stem and Lena tributaries and C emission fluxes*

260 The main hydrological C parameters of the Lena River and its tributaries ( $\text{pCO}_2$ ,  $\text{CH}_4$ , pH, DIC,  
261 and DOC) are listed in **Tables 1 and 2**. Continuous  $\text{pCO}_2$  measurements in the main stem (4285  
262 individual data points) averaged for each 20 km interval over the full distance of the boat route  
263 demonstrated a sizable increase (from ca. 380 to 1040  $\mu\text{atm}$ ) in  $\text{pCO}_2$  northward (**Fig. 2**). There was a  
264 positive correlation between the  $\text{pCO}_2$  and distance from the head waters of the Lena River ( $r = 0.625$ ,  $p$   
265  $< 0.01$ , **Fig. 3 A**). The  $\text{CH}_4$  concentration was low ( $0.054 \pm 0.023$  and  $0.061 \pm 0.028 \mu\text{mol L}^{-1}$  in the Lena  
266 River and 20 tributaries, respectively) and did not change appreciably along the main stem and among  
267 the 20 tributaries (**Fig. 3 B**). The DOC concentration did not demonstrate any systematic variations over  
268 the main stem ( $10.5 \pm 2.4 \text{ mg L}^{-1}$ , **Fig. 3 C**), however it was higher and more variable in tributaries ( $15.8$   
269  $\pm 8.6 \text{ mg L}^{-1}$ ). The DIC concentration decreased about five-fold from the head waters to the middle course  
270 of the Lena River (**Fig. 3 D**), and pH decreased by 0.8 units downstream (**Fig. 3 E**).

271 Generally, the concentrations of DOC measured in the present study during the peak of the spring  
272 flood are at the highest range of previous assessments during summer baseflow (around 5 mg L<sup>-1</sup>; range  
273 of 2 to 12 mg L<sup>-1</sup>, Cauwet and Sidorov, 1996; Lara et al., 1998; Lobbes et al., 2000; Kuzmin et al., 2009;  
274 Kutscher et al., 2017). The DIC concentration in the main stem during spring flood was generally lower  
275 than that reported during summer baseflow (around 10 mg L<sup>-1</sup>; range of 5 to 50 mg L<sup>-1</sup>) but consistent  
276 with values reported in Yakutsk during May and June period (7 to 20 mg L<sup>-1</sup>, Sun et al., 2018). A sizable  
277 decrease in DIC concentration between the headwaters (first 500 km of the river) and the Lena River  
278 middle course was also consistent with the alkalinity pattern reported in previous works during summer  
279 baseflow (Pipko et al., 2010; Semiletov et al., 2011). For the Lena river tributaries, the most  
280 comprehensive data set on major ions was acquired in July-August of 1991-1996 by Huh and Edmond's  
281 group (Huh and Edmond, 1999; Huh et al., 1998a, b) and by Sun et al. (2018) in July 2012 and at the end  
282 of June 2013. For most tributaries, the concentration of DIC was a factor of 2 to 5 lower during spring  
283 flood compared to summer baseflow. This result can be explained by the strong dilution of carbonate-  
284 rich groundwaters feeding the river in spring high flow compared to summer low flow.

285 The measured pCO<sub>2</sub> in the river water and published (Karlsson et al., 2021) gas transfer  
286 coefficient (4.46 m d<sup>-1</sup>) allowed for calculation of the CO<sub>2</sub> fluxes over the full length of the studied main  
287 stem (2600 km) and the sampled tributaries. Calculated CO<sub>2</sub> fluxes of the main stem and tributaries  
288 ranged from zero and slightly negative (uptake) values in the most southern part of the Lena River and  
289 certain tributaries (N Katyma), to between 0.5-2.0 g C m<sup>-2</sup> d<sup>-1</sup> in the rest of the main stem and tributaries  
290 (**Tables 1, 2; Fig. 2 B**). The largest part of the Lena River main stem, 1429 km from Kirenga to Tuolba,  
291 exhibited quite stable flux of 1.1±0.2 g C m<sup>-2</sup> d<sup>-1</sup>. In the last ~400 km part of the Lena River main stem  
292 studied in this work, from Tuolba to Aldan, the calculated fluxes increased to 1.7±0.08 g C m<sup>-2</sup> d<sup>-1</sup>.

293 The river water concentrations of dissolved CH<sub>4</sub> in the tributaries and the main channel  
294 (0.059±0.006; IQR range from 0.025 to 0.199 μmol L<sup>-1</sup>, **Table 1, 2**) did not exhibit any trend with  
295 distance from headwaters or landscape parameters of the catchments. These values are consistent with  
296 the range of CH<sub>4</sub> concentration in the low reaches of the Lena River main channel (0.03-0.085 μmol L<sup>-1</sup>

297 <sup>1</sup>; Bussman, 2013) and are 100-500 times lower than those of CO<sub>2</sub>. Consequently, diffuse CH<sub>4</sub> emissions  
298 constituted less than 1 % of total C emissions and are not discussed in further detail.

299

### 300 *3.2. Diurnal (night/day) pCO<sub>2</sub> variations and spatial variations across the river transect*

301 The diel continuous CO<sub>2</sub> measurements of 3 tributaries (Kirenga, Tuolba and Aldan) and 14 sites  
302 of the Lena River main channel showed generally modest variation with diurnal range within 10 % of  
303 the average pCO<sub>2</sub> (**Fig. 4** and **Fig. S2**). The observed variations in pCO<sub>2</sub> between day and night were not  
304 linked to water temperature ( $p > 0.05$ ), which did not vary more than 1-2 °C between the day and night  
305 period.

306 The spatial variations of hydrochemical parameters were tested in the upper reaches of the Lena  
307 main stem and its largest tributary - the Aldan River (**Fig. S3**). In the Lena River, over a lateral distance  
308 of 550 m across the river bed, the pCO<sub>2</sub> and CH<sub>4</sub> concentrations were equal to  $569 \pm 4.6 \mu\text{atm}$  and  
309  $0.0406 \pm 0.0074 \mu\text{mol L}^{-1}$ , respectively, whereas the DIC and DOC concentrations varied  $< 15\%$  ( $n = 5$ ).  
310 In the Aldan River, over a 2700 m transect across the flow, the pCO<sub>2</sub> and CH<sub>4</sub> concentrations were equal  
311 to  $1035 \pm 95 \mu\text{atm}$  and  $0.078 \pm 0.00894 \mu\text{mol L}^{-1}$ , respectively, whereas DIC and DOC varied within  $< 20\%$   
312 ( $n = 4$ ). Overall, these results supported our design of punctual (snap shot) sampling in the middle of the  
313 river.

314

### 315 *3.3. Impact of catchment characteristics on pCO<sub>2</sub> in tributaries of the Lena River*

316 The CO<sub>2</sub> concentration in the Lena River main stem and tributaries increased from southwest to  
317 northeast (**Table 1, 2; Fig. 2**), and this was reflected in a positive ( $R = 0.66$ ) correlation between CO<sub>2</sub>  
318 concentration and continuous permafrost coverage and a negative ( $R = -0.76$ ) correlation with MAAT  
319 (**Table 3**). Among different landscape factors, C stock in upper 0-30 and 0-100 cm of soil, the proportion  
320 of riparian vegetation and bare rocks, the coverage by deciduous needle-leaf forest, and coverage of river  
321 watershed by water bodies (mostly lakes) exhibited significant ( $p < 0.01$ ,  $n = 19$ ) positive correlations  
322 ( $0.54 \leq R \leq 0.86$ ) with average pCO<sub>2</sub> of the Lena River tributaries (**Fig. 5**). The other potentially important  
323 landscape factors of the river watershed (proportion of peatland and bogs, tundra coverage, total

324 aboveground vegetation, type of permafrost, annual precipitation) did not significantly impact the CO<sub>2</sub>  
325 concentration in the Lena River tributaries (**Table 3**).

326 Further assessment of landscape factor control on C parameters of the river water was performed  
327 via a PCA. This analysis basically confirmed the results of linear regressions and revealed two factors  
328 capable explaining only 12.5 and 3.5% of variability (**Fig. S4**). The F1 strongly acted on the sample  
329 location at the Lena transect, the content of OC in soils, the watershed coverage by deciduous needle-  
330 leaf forest and shrubs, riparian vegetation (a proxy for the width of the riparian zone), but also proportion  
331 of tundra, bare rock and soils, water bodies, peatland and bogs (> 0.90 loading). The pCO<sub>2</sub> was  
332 significantly linked to F1 (0.72 loading).

333

#### 334 *3.4. Areal emission from the Lena River basin*

335 The areal emission of CO<sub>2</sub> from the lotic waters of the Lena River watershed were assessed based  
336 on total river water coverage of the Lena basin in 2016 (28,197 km<sup>2</sup>, of which 5,022 km<sup>2</sup> is seasonal  
337 water, according to the Global SDG database). This value is consistent with the total river surface area  
338 from the GRWL Mask database (22,479 km<sup>2</sup>). Given that the measurements were performed at the peak  
339 of spring flood in 2016, we used the maximal water coverage of the Lena River basin.

340 Based on past calculated pCO<sub>2</sub> of the Lena River (400 - 1000 μatm, Semiletov, 1999; Semiletov  
341 et al., 2011; Pipko et al., 2010) both the seasonality and spatial differences downstream are relatively  
342 small. Indeed, for the lower reaches of the Lena River, from Yakutsk to the Lena Delta, Semiletov (1999)  
343 and Semiletov et al. (2011) reported, for August-September 1995, the average pCO<sub>2</sub> of 538±96 μatm  
344 (range 380-727 μatm). This value is very similar to the one obtained in July 2003 for the low reaches of  
345 Lena (559 μatm, Pipko et al., 2010). Over the full length of the Lena River, from Ust-Kut to the Lena  
346 mouth, Pipko et al. (2010) reported an average pCO<sub>2</sub> of 450 ± 100 μatm in June-July 2003. At the same  
347 time, calculated pCO<sub>2</sub> from previous field campaigns are generally lower than the pCO<sub>2</sub> of the Lena  
348 River main stem directly measured in this study: 700-800 μatm for the Ust Kut – Nuya segment (1331  
349 km); 845 – 1050 μatm for the Nuya – Aldan segment (1050 km).

350 Thus, despite the absolute values of calculated pCO<sub>2</sub> involving uncertainties (our calculated:  
351 measured pCO<sub>2</sub> in Lena River main channel and tributaries equaled 0.67±0.15 (n = 47)), this suggests  
352 spatial and temporal stability of the pCO<sub>2</sub> in the Lena River waters and allows for extrapolation of the  
353 measured pCO<sub>2</sub> in the Lena River from Yakutsk to Aldan to the lower reaches of the river. As for the  
354 Lena tributaries, to the best of our knowledge there is no published information on pCO<sub>2</sub> concentration  
355 and emission. Overall, the major uncertainty in estimation of the Lena River basin emission stems from  
356 a lack of direct pCO<sub>2</sub> measurements in the northern part of the main channel over ca. 1000 km  
357 downstream of the Aldan River including the large tributary Vilyi. Further, we noted that the largest  
358 northern tributary, the Aldan River providing 70% of the spring time discharge of the Lena River (Pipko  
359 et al., 2010), demonstrated sizably higher emissions compared to the Lena River main channel upstream  
360 of Aldan (3.2±0.5 and 1.69±0.08 g C m<sup>-2</sup> d<sup>-1</sup>, respectively).

361 For areal emission calculations, we used the range of CO<sub>2</sub> emissions from 1 to 2 g C m<sup>-2</sup> d<sup>-1</sup> which  
362 covers full variability of both large and small tributaries and the Lena River main channel (**Tables 1-2,**  
363 **Figure 2 B**). This estimation assumes lack of pCO<sub>2</sub> dependence on the size of the watershed in the Lena  
364 basin as confirmed by our data (**Fig. S5**). For an alternative areal emission calculations, we explicitly  
365 took into account the water area of the main stem (43% relative to the total water area of the Lena  
366 catchment) and we introduced the partial weight of emission from the 3 largest tributaries (Aldan,  
367 Olekma and Vitim) according to their catchment surface areas (43, 12 and 14% of all sampled territory,  
368 respectively). We summed up contribution of the Lena river main stem and the tributaries and we  
369 postulated the average emission from the main stem upstream of Aldan (1.25±0.30 g C m<sup>-2</sup> d<sup>-1</sup>) as  
370 representative of the whole Lena River. This resulted in an updated value of 1.65±0.5 g C m<sup>-2</sup> d<sup>-1</sup> which  
371 is within the range of 1 to 2 g C m<sup>-2</sup> d<sup>-1</sup> assessed previously. Note that this value is most likely  
372 underestimated because emissions from the main stem downstream of Aldan are at least 10 % higher  
373 (Table 1, Fig. 1 B).

374 For the two months of maximal water flow (middle of May - middle of July), the C emission from  
375 the whole Lena basin equates to 2.8 ± 0.85 Tg C which is 20 to 30% of the DOC and DIC lateral export  
376 to the Arctic Ocean. Assuming six months of open water period and no emission during winter, this

377 yields  $8.3 \pm 2.5 \text{ Tg C y}^{-1}$  of annual emission for the whole Lena River basin (2,490, 000 km<sup>2</sup>) with a total  
378 lotic water area of 28,100 km<sup>2</sup>. Considering the only 23,200 km<sup>2</sup> water area in July-October (and maximal  
379 water coverage in May-June), these numbers decrease by 12% which is below the uncertainties  
380 associated with our evaluation.

381

382

## 383 **4. DISCUSSION**

### 384 *4.1. Possible driving factors of CO<sub>2</sub> pattern in the Lena River basin*

385 Generally, the SW to NE increase in CO<sub>2</sub> concentrations and fluxes of the tributaries was  
386 consistent with CO<sub>2</sub> pattern in the main stem (**Fig. 2; Tables 1, 2**), and thus can be considered as a  
387 specific feature of CO<sub>2</sub> exchange between lotic waters and atmosphere in the studied part of the Lena  
388 Basin. At the same time, there were sizable local variations (peaks) in CO<sub>2</sub> concentration of the main  
389 stem along the sampling route (**Fig. 2 A**). Peaks shown on the diagram of the main stem are not  
390 necessarily linked to CO<sub>2</sub>-rich tributaries, but likely reflect local processes in the main stem, including  
391 lateral influx from the shores and shallow subsurface waters, which is typical for permafrost regions of  
392 forested Siberian watersheds (i.e., Bagard et al., 2011). Given that the data were averaged over ~20-km  
393 distance, we believe that these peaks are not artifacts but reflect local heterogeneity of the pCO<sub>2</sub> pattern  
394 in the main stem (turbulences, suprapermafrost water discharge, sediment resuspension and respiration).  
395 Note that such a heterogeneity was not observed in the tributaries, at least at the scale of our spatial  
396 coverage (see **Fig. S1 B, S3**).

397 The PCA demonstrated extremely low ability to describe the data variability (12% by F1 and only  
398 3.5% by F2). We believe that the most likely reason of weak PCA capacity is the rather homogeneous  
399 distribution of CO<sub>2</sub> and CH<sub>4</sub> among the tributaries, primarily linked to the specific hydrological period,  
400 studied in this work - the spring flood. During this high flow period, the local lithological and soil  
401 heterogeneities among tributaries or the segments of the main stem virtually disappear and surface flow  
402 (via vegetation leaching) becomes the most important driver of riverine chemistry, as is known from

403 adjacent permafrost territories in Central Siberia (i.e., Bagard et al., 2011). Nevertheless, some specific  
404 features of the data structure could be established. The first factor, significantly linked to pCO<sub>2</sub> (0.72  
405 loading), strongly acted on the sample location at the Lena transect, the watershed coverage by deciduous  
406 needle-leaf forest and shrubs, riparian vegetation, and also the proportion of tundra, bare rock and soils,  
407 water bodies, peatland and bogs (> 0.90 loading). This is fully consistent with spatial variation of pCO<sub>2</sub>  
408 along the permafrost and climate gradient in the main channel and sampled tributaries. Positive loading  
409 of riparian vegetation, peatlands and bogs on F1 (0.927 and 0.989, respectively) could reflect a  
410 progressive increase in the feeding of the river basin by mire waters, an increase in the proportion of  
411 needle-leaf deciduous trees, and in the width of the riparian zone from the SW to the NE direction.

412         Lack of sizable variation in pCO<sub>2</sub> between the day and night period or across the river bed  
413 suggests quite low site-specific and diurnal variability. It may be indicative of a negligible role of primary  
414 productivity in the water column given the low water temperatures, shallow photic layer of organic-rich  
415 and turbid waters and lack of periphyton activity during high flow of the spring flood. The pCO<sub>2</sub>  
416 increased by a factor of 2 to 4 along the permafrost/temperature gradient from the southwest to the  
417 northeast, for both the main channel and sampled tributaries. This may reflect progressive increase in the  
418 feeding of the river basin by mire waters, increase in the proportion of needle-leaf deciduous forest, and  
419 an increase in the width of the riparian zone. Another strong correlation is observed between the stock of  
420 OC in soils (both 0-30 and 0-100 cm depth) and the pCO<sub>2</sub> of Lena tributaries. Organic-rich soils are  
421 widely distributed in the central and northern part of the basin. The most southern part of the Lena basin  
422 is dominated by carbonate rocks and crystalline silicates in generally mountainous terrain, where only  
423 thin mineral soils are developed. The northern (downstream of the Olekma River) part of the basin  
424 consists of soils developed on sedimentary silicate rocks as well as vast areas of easily eroded yedoma  
425 soils. It is likely that both organic matter mineralization in OC-rich permafrost soils and lateral export of  
426 CO<sub>2</sub> from these soils, together with particulate and dissolved OC export and mineralization in the water  
427 column, are the main sources of CO<sub>2</sub> in the river water. Although some studies have demonstrated high  
428 lability of DOM in arctic waters (Cory et al., 2014; Ward et al., 2017; Cory and Kling, 2018), others  
429 suggest it is low and does not support the major part of CO<sub>2</sub> supersaturation in water (Shirokova et al.,

430 2019; Payandi-Rolland et al., 2020; Laurion et al., 2021). Note that we have not observed any significant  
431 relationship between the DOC and pCO<sub>2</sub> in the Lena River and tributaries (**Fig. S6 A**). Lack of such a  
432 correlation and absence of diurnal pCO<sub>2</sub> variations imply that in-stream processing of dissolved terrestrial  
433 OC is not the main driver of CO<sub>2</sub> supersaturation in the river waters of the Lena River basin. Furthermore,  
434 a lack of lateral (across the river bed) variations in pCO<sub>2</sub> does not support a sizable input of soil waters  
435 from the shore, although we admit that much higher spatial coverage along the river shore is needed to  
436 confirm this hypothesis.

437         The role of underground water discharge in regulating pCO<sub>2</sub> pattern of the tributaries is expected  
438 to be most pronounced in the SW part of the basin (Lena headwaters), where carbonate rocks of the  
439 basement would provide sizable amounts of CO<sub>2</sub> discharge in the river bed. However, there was no  
440 relationship between the proportion of carbonate rocks on the watershed and the pCO<sub>2</sub> in the tributaries  
441 (**Fig. S6 B**). Furthermore, for the Lena River main stem, the lowest CO<sub>2</sub> concentrations were recorded in  
442 the upper reaches (first 0-800 km) where carbonate rocks dominate. Altogether, this makes the impact of  
443 CO<sub>2</sub> from underground carbonate reservoirs on river water CO<sub>2</sub> concentrations unlikely. This is further  
444 illustrated by a lack of correlation between pCO<sub>2</sub> and DIC or pH (**Fig. S7 A** of the Supplement). The pH  
445 did not control the CO<sub>2</sub> concentration in the main stem and only weakly impacted the CO<sub>2</sub> in the  
446 tributaries (**Fig. S7 B**). The latter could reflect an increase in pCO<sub>2</sub> in the northern tributaries which  
447 exhibited generally lower pH compared to the SW tributaries hosted within the carbonate rocks. Overall,  
448 such low correlations of CO<sub>2</sub> with DIC and pH reflected a generally low predictive capacity to calculate  
449 pCO<sub>2</sub> from measured pH, temperature and alkalinity (see section 3.4).

450         Therefore, other sources of riverine CO<sub>2</sub> may include particulate organic carbon processing in the  
451 water column (Attermeyer et al., 2018), river sediments (Humborg et al., 2010) and within the riparian  
452 zone (Leith et al., 2014, 2015) which require further investigation. In addition, although there was no  
453 sizable variation in pCO<sub>2</sub> between the day and night period or across the river bed, the flux could show  
454 different spatial and temporal patterns if *k* shows larger variability (cf., Beaulieu et al., 2012). This calls  
455 for a need of direct flux measurements in representative rivers and streams of the Lena River basin.  
456 Overall, the present study demonstrates highly dynamic and non-equilibrium behavior of CO<sub>2</sub> in the river

457 waters, with possible *hot spots* from various local sources. For these reasons, *in-situ*, high spatial  
458 resolution measurements of CO<sub>2</sub> concentration in rivers—such as those reported for the Lena Basin in  
459 this study—are crucially important for quantifying the C emission balance in lotic waters of high  
460 latitudes.

461

#### 462 *4.2. Areal emission from the Lena River basin vs lateral export to the Arctic Ocean*

463 The estimated CO<sub>2</sub> emissions from the Lena River main channel over 2600 km distance (0.8 –  
464 1.7 g C m<sup>-2</sup> d<sup>-1</sup>) are comparable to values directly measured in rivers and streams of the continuous  
465 permafrost zone of western Siberia (0.98 g C m<sup>-2</sup> d<sup>-1</sup>, Serikova et al., 2018), the Kolyma River (0.35 g C  
466 m<sup>-2</sup> d<sup>-1</sup> in the main stem; 2.1 g C m<sup>-2</sup> d<sup>-1</sup> for lotic waters of the basin), and the Ob River main channel  
467 (1.32±0.14 g C m<sup>-2</sup> d<sup>-1</sup> in the permafrost-free zone, Karlsson et al., 2021). At the same time, the Lena  
468 River flux (FCO<sub>2</sub>) values are lower than typical emissions from running waters in the contiguous United  
469 States (3.1 g C m<sup>-2</sup> d<sup>-1</sup>, Hotchkiss et al., 2015), small mountain streams in Northern Europe (3.3 g C m<sup>-2</sup>  
470 d<sup>-1</sup>, Rocher-Ros et al., 2019), and small streams of the northern Kolyma River (6 to 7 g C m<sup>-2</sup> d<sup>-1</sup>, Denfeld  
471 et al., 2013) and Ob River in the permafrost-affected zone (3.8 to 5.4 g C m<sup>-2</sup> d<sup>-1</sup>, Karlsson et al., 2021).  
472 In contrast to the main stem, the range of FCO<sub>2</sub> in the tributaries is larger (0.2 to 3.2 g C m<sup>-2</sup> d<sup>-1</sup>) and  
473 presumably reflects a strong variability in environmental conditions across a sizable landscape and  
474 climate transect.

475 Total C emissions from other major Eastern Eurasian permafrost-draining rivers (i.e. sum of  
476 Kolyma, Lena and Yenisei rivers) based on indirect estimates (40 Tg C y<sup>-1</sup>, Raymond et al., 2013) are  
477 generally supportive of the estimations of the Lena River in this study (5 to 10 Tg C y<sup>-1</sup>). At the same  
478 time, the C emission from the Lena river basin (28,100 km<sup>2</sup> water area) are lower than those of the lotic  
479 waters of western Siberia (30 Tg C y<sup>-1</sup> for 33,389 km<sup>2</sup> water area, Karlsson et al., 2021). The latter drain  
480 through thick, partially frozen peatlands within the discontinuous, sporadic and permafrost-free zones,  
481 which can cause high OC input and processing and, thus, enhanced C emissions (Serikova et al., 2018).

482 Despite the high uncertainty on our regional estimations [due to lack of directly measured gas  
483 transfer values and low seasonal resolution] we believe that these estimations are conservative and can

484 be considered as first order values pending further improvements. In order to justify extrapolation of our  
485 data to all seasons and the entire area of the Lena basin, we analyzed data for spatial and temporal  
486 variations in pCO<sub>2</sub> of the Lena River main stem from available literature. From the literature there were  
487 three important findings. First, based on published data, the seasonal and spatial variabilities of pCO<sub>2</sub>  
488 across the majority of the Lena River main stem are not high during open water period, although the low  
489 reaches of the Lena River may exhibit higher emissions compared to the middle and upper course (see  
490 **section 3.4**). Second, although small mountainous headwater streams of the tributaries may exhibit high  
491 *k* due to turbulence, this could be counteracted by lower CO<sub>2</sub> supply from low OC in mineral soil, lack  
492 of riparian zone and scarce vegetation. Third, although these small streams (watershed area < 100 km<sup>2</sup>)  
493 may represent > 60% of total watershed surfaces of the Lena basin (Ermolaev et al., 2018), their  
494 contribution to the total water surface is < 20% (19% from combined analysis of DEM GMTED2010 and  
495 16% from the GRWL or Global SDG database as estimated in this study). Therefore, given that (i) within  
496 the stream-river continuum, the CO<sub>2</sub> efflux increases only two-fold demonstrating a discharge decrease  
497 by a factor of 10,000 (from 100 to 0.01 m<sup>3</sup> s<sup>-1</sup>, Hotchkiss et al., 2015), and (ii) the watershed area had no  
498 impact on pCO<sub>2</sub> in the river water (**Fig. S5**), this uncertainty is likely less important. As such, instead of  
499 integrating indirect literature data, we used the pCO<sub>2</sub> values measured in the present study to calculate  
500 the overall CO<sub>2</sub> emission from all lotic waters of the Lena basin.

501 The C evasion from the Lena basin assessed in the present work is comparable to the total  
502 (DOC+DIC) lateral export by the Lena River to the Arctic Ocean (10 Tg C y<sup>-1</sup> by Semiletov et al. (2011),  
503 or 11 Tg C y<sup>-1</sup> (5.35 Tg DIC y<sup>-1</sup> + 5.71 Tg DOC y<sup>-1</sup> by Cooper et al. (2008)). Moreover, the C evasion  
504 strongly exceeds sedimentary C input to the Laptev Sea by all Siberian rivers (1.35 Tg C y<sup>-1</sup>, Rachold et  
505 al. (1996) and Dudarev et al. (2006)), the Lena River annual discharge of particulate organic carbon (0.38  
506 Tg y<sup>-1</sup>, Semiletov et al., 2011), and OC burial on the Kara Sea Shelf (0.37 Tg C y<sup>-1</sup>, Gebhardt et al., 2005).

507 Typical concentrations of CH<sub>4</sub> in the Lena tributaries and the main channel are 100 to 500 times  
508 lower than those of CO<sub>2</sub>. Given that the global warming potential (GWP) of methane on a 100-year scale  
509 is only 25 times higher than that of CO<sub>2</sub>, the long-term role of diffuse methane emission from the Lena  
510 River basin is still 4 to 20 times lower than that of CO<sub>2</sub>. However, on a short-term scale (20 years), the

511 GWP of methane can be as high as 96 (Alvarez et al., 2018) and its role in climate regulation becomes  
512 comparable to that of the CO<sub>2</sub>. This has to be taken into account for climate modeling of the region.

513 The follow up studies of this large heterogenous and important system should include CO<sub>2</sub>  
514 measurements in 1) the low reaches of the Lena River, downstream of Aldan, notably large organic-rich  
515 tributaries such as Vilyi (454,000 km<sup>2</sup>) and where the huge floodzone (20-30 km wide) with large number  
516 of lakes and wetlands is developed, and 2) highly turbulent eastern tributaries of the Lena River  
517 downstream of Aldan, which drain the Verkhoyansk Ridge and are likely to exhibit elevated gas transfer  
518 coefficients.

519

## 520 **5. Conclusions**

521 Continuous pCO<sub>2</sub> measurements over 2600 km of the upper and middle part of the Lena River  
522 main channel and 20 tributaries during the peak of spring flood allowed to quantify, for the first time, in-  
523 situ pCO<sub>2</sub> variations which ranged from 500 to 1700 μatm and exhibited a 2 to 4-fold increase in CO<sub>2</sub>  
524 concentration northward. There was no major variation in pCO<sub>2</sub> between the day and night period or  
525 across the river bed which supports the chosen sampling strategy. The northward increase in pCO<sub>2</sub> was  
526 correlated with an increased proportion of needle-leaf deciduous trees, the width of the riparian zone and  
527 the stock of organic C in soils. Among the potential drivers of riverine pCO<sub>2</sub>, changes in the vegetation  
528 pattern (northward migration of larch tree line in Siberia; Kruse et al., 2019) and soil OC stock are likely  
529 to be most pronounced during ongoing climate warming and thus the established link deserves further  
530 investigation. The total C emission from the lotic waters of the Lena River basin ranges from 5 to 10 Tg  
531 C y<sup>-1</sup> which is comparable to the annual lateral export (50% DOC, 50 % DIC) by the Lena River to the  
532 Arctic Ocean. However, these preliminary estimations of C emission should be improved by direct flux  
533 measurements across seasons in different types of riverine systems of the basin, notably in the low  
534 reaches of the Lena River.

535

536

537

538 **Acknowledgements.**

539 We acknowledge support from an RSF grant 18-17-00237\_P, the Belmont Forum Project VULCAR-  
540 FATE, and the Swedish Research Council (no. 2016-05275). We thank the Editor Ji-Hyung Park and 3  
541 anonymous reviewers for their very constructive comments. Chris Benker is thanked for English  
542 editing.

543

544 **Authors contribution.**

545 SV and OP designed the study and wrote the paper; SV, YK and OP performed sampling, analysis and  
546 their interpretation; MK performed landscape characterization of the Lena River basin and calculated  
547 water surface area; JK provided analyses of literature data, transfer coefficients for FCO<sub>2</sub> calculations  
548 and global estimations of areal emission vs export.

549

550 **Competing interests.**

551 The authors declare that they have no conflict of interest.

552

553 **References**

- 554 Abril, G., Bouillon, S., Darchambeau, F., Teodoru, C. R., Marwick, T. R., Tamooh, F., Ochieng Omengo,  
555 F., Geeraert, N., Deirmendjian, L., Polsenaere, P., and Borges, A. V.: Technical Note: Large  
556 overestimation of pCO<sub>2</sub> calculated from pH and alkalinity in acidic, organic-rich freshwaters,  
557 *Biogeosciences*, 12, 67–78, <https://doi.org/10.5194/bg-12-67-2015>, 2015.
- 558 Ahmed, R., Prowse, T., Dibike, Y., Bonsal, B., and O’Neil H.: Recent trends in freshwater influx to the  
559 Arctic Ocean from four major Arctic-draining rivers, *Water*, 12, 1189; doi:10.3390/w12041189,  
560 2020.
- 561 Alin, S. R., Rasera, M. F. F. L., Salimon, C. I., Richey, J. E., Holtgrieve, G. W., Krusche, A. V., et al. :  
562 Physical controls on carbon dioxide transfer velocity and flux in low-gradient river systems and  
563 implications for regional carbon budgets. *J. Geophys. Res. Biogeosci.* 116, G01009. doi:  
564 10.1029/2010jg001398, 2011.
- 565 Allen, G. H. and Pavelsky, T. M.: Global extent of rivers and streams, *Science* 361, 585-58,  
566 doi:10.1126/science.aat0636, 2018.
- 567 Alvarez, R. A., Zavala-Araiza, D., Lyon, D. R., Allen, D. T., Barkley, Z. R., Brandt, A. R., Davis, K.  
568 J., Herndon, S. C., Jacob, D. J., Karion, A., Kort, E. A., Lamb, B. K., Lauvaux, T., Maasakkers, J.  
569 D., Marchese, A. J., Omara, M., Pacala, S. W., Peischl, J., Robinson, A. L., Shepson, P. B., Sweeney,  
570 C., Townsend-Small, A., Wofsy, S. C., Hamburg, S. P.: Assessment of methane emissions from the  
571 U.S. oil and gas supply chain. *Science* 361, 186–188, doi:10.1126/science.aar7204, 2018.
- 572 Attermeyer, K., Catalan, N., Einarsdottir, K., Freixa, A., Groeneveld, M., Hawkes, J. A., et al.: Organic  
573 carbon processing during transport through boreal inland waters: particles as important sites, *J.*  
574 *Geophys. Res. - Biogeosci.* 123, 2412–2428, doi:10.1029/2018JG004500, 2018.
- 575 Bagard, M. L., Chabaux, F., Pokrovsky, O. S., Viers, J., Prokushkin, A. S., Stille, P., Rihs, S., Schmitt,  
576 A. D., Dupre, B.: Seasonal variability of element fluxes in two Central Siberian rivers draining  
577 high latitude permafrost dominated areas. *Geochim. Cosmochim. Acta* 75, 3335-3357, 2011.
- 578 Bartalev, S. A., Egorov, V. A., Ershov, D. V., Isaev, A. S., Lupyan, E. A., Plotnikov, D. E., and Uvarov,  
579 I. A.: Remote mapping of vegetation land cover of Russia based on data of MODIS  
580 spectroradiometer, *Modern Problems of Earth Remote Sensing from Space*, 8 (No 4), 285-302.  
581 [http://d33.infospace.ru/d33\\_conf/2011v8n4/285-302.pdf](http://d33.infospace.ru/d33_conf/2011v8n4/285-302.pdf), 2011.

- 582 Beaulieu, J. J., Shuster, W. D., and Rebholz, J. A.: Controls on gas transfer velocities in a large river, *J.*  
583 *Geophys. Res.*, 117, G02007, doi:10.1029/2011JG001794, 2012.
- 584 Berezovskaya, S., Yang, D., and Hinzman, L.: Long-term annual water balance analysis of the Lena  
585 River, *Glob. Planet. Change* 48, 84–95, <https://doi.org/10.1016/j.gloplacha.2004.12.006>, 2005.
- 586 Brown, J., Ferrians Jr., O. J., Heginbottom, J. A., and Melnikov, E. S.: Circum-Arctic Map of Permafrost  
587 and Ground Ice Conditions. National Snow and Ice Data Center/World Data Center for Glaciology,  
588 Boulder, CO, USA, Digital media, 2002.
- 589 Bussmann I.: Distribution of methane in the Lena Delta and Buor-Khaya Bay, Russia, *Biogeosciences*  
590 10, 4641–4652, <https://doi.org/10.5194/bg-10-4641-2013>, 2013.
- 591 Cai, W.-J. and Wang, Y.: The chemistry, fluxes, and sources of carbon dioxide in the estuarine waters of  
592 the Satilla and Altamaha Rivers, Georgia, *Limnol. Oceanogr.* 43, 657–668.  
593 <https://doi.org/10.4319/lo.1998.43.4.0657>, 1998.
- 594 Cauwet, G., and Sidorov I.: The biogeochemistry of Lena River: organic carbon and nutrients  
595 distribution, *Marine Chem.* 53, 211–227, [https://doi.org/10.1016/0304-4203\(95\)00090-9](https://doi.org/10.1016/0304-4203(95)00090-9), 1996.
- 596 Chadburn, S. E., Krinner, G., Porada, P., Bartsch, A., Beer C. et al.: Carbon stocks and fluxes in the high  
597 latitudes: using site-level data to evaluate Earth system models, *Biogeosciences* 14(22), 5143–5169,  
598 <https://doi.org/10.5194/bg-14-5143-2017>, 2017.
- 599 Chevychelov, A. P., and Bosikov, N. P.: Natural Conditions, in: *The Far North*, edited by E.I. Troeva et  
600 al., pp. 123, Springer, Netherlands, [https://link.springer.com/chapter/10.1007/978-90-481-3774-](https://link.springer.com/chapter/10.1007/978-90-481-3774-9_1)  
601 [9\\_1](https://link.springer.com/chapter/10.1007/978-90-481-3774-9_1), 2010.
- 602 Cooper, L. W., McClelland, J. W., Holmes, R. M., Raymond, P. A., Gibson, J. J., Guay, C. K., and  
603 Peterson, B. J.: Flow-weighted values of runoff tracers ( $\delta^{18}\text{O}$ , DOC, Ba, alkalinity) from the six  
604 largest Arctic rivers, *Geophys. Res. Lett.*, 35, L18606, doi:10.1029/2008GL035007, 2008.
- 605 Cory, R. M., Ward, C. P., Crump, B. C., and Kling, G. W.: Sunlight controls water column processing  
606 of carbon in arctic fresh waters, *Science*, 345, 925–928, doi: 10.1126/science.1253119, 2014.
- 607 Cory, R. M., Kling, G. W.: Interactions between sunlight and microorganisms influence dissolved  
608 organic matter degradation along the aquatic continuum, *Limnol. Oceanogr. Lett.*, 3, 102–116,  
609 <https://doi.org/10.1002/lo2.10060>, 2018.
- 610 Crawford, J. T., Loken, L. C., Casson, N. J., Smith, C., Stone, A. G, and Winslow, L. A.: High-speed  
611 limnology: using advanced sensors to investigate spatial variability in biogeochemistry and  
612 hydrology, *Environ. Sci. Technol.* 2015, 49, 1, 442–450, <https://doi.org/10.1021/es504773x>,  
613 2015.
- 614 Denfeld, B.A., Frey K.E., Sobczak, W.V., Mann P.J., and Holmes, R.M.: Summer CO<sub>2</sub> evasion from  
615 streams and rivers in the Kolyma River basin, north-east Siberia, *Polar Res.*, 32, Art No 19704,  
616 <https://doi.org/10.3402/polar.v32i0.19704>, 2013.
- 617 Denfeld, B. A., Baulch, H. M., del Giorgio, P. A., Hampton, S. E., and Karlsson, J.: A synthesis of  
618 carbon dioxide and methane dynamics during the ice-covered period of northern lakes,  
619 *Limnology and Oceanography Letters* 3, 117–131, doi:10.1002/lo2.10079, 2018.
- 620 Dudarev, O. V., Semiletov, I. P., and Charkin, A. N.: Particulate material composition in the Lena River  
621 - Laptev Sea system: Scales of heterogeneities, *Doklady Earth Sciences*, 411A (9), 1445–1451,  
622 <https://link.springer.com/content/pdf/10.1134/S1028334X0609025X.pdf>, 2006.
- 623 Ermolaev, O. P., Maltzev K. A., Mukharamova S. S., Khomyakov P. V., and Shynbergenov E. A.:  
624 Cartographic model of small rivers of the Lena River basin. *Ychenue Zapiski Kazansky Univ.*,  
625 *Ser. Natural Sciences*, 160(1), 126–144, [https://cyberleninka.ru/article/n/kartograficheskaya-](https://cyberleninka.ru/article/n/kartograficheskaya-model-basseynovyh-geosistem-malyh-rek-vodosbora-reki-leny/viewer)  
626 [model-basseynovyh-geosistem-malyh-rek-vodosbora-reki-leny/viewer](https://cyberleninka.ru/article/n/kartograficheskaya-model-basseynovyh-geosistem-malyh-rek-vodosbora-reki-leny/viewer), 2018.
- 627 Feng, X. J., Vonk, J. E., van Dongen, B. E., Gustafsson, O., Semiletov, I. P., Dudarev, O. V., Wang, Z.  
628 H., Montlucon, D. B., Wacker, L., and Eglinton, T.I.: Differential mobilization of terrestrial carbon  
629 pools in Eurasian Arctic river basins, *P. Natl. Acad. Sci. USA*, 110, 14168–14173,  
630 <https://doi.org/10.1073/pnas.1307031110>, 2013.
- 631 Frey, K. E., and Smith, L.C.: Amplified carbon release from vast West Siberian peatlands by 2100,  
632 *Geophys. Res. Lett.*, 32, L09401, doi:10.1029/2004GL022025, 2005.
- 633 Gautier, E., Depret, T., Costard, F., Vermoux, C., Fedorov, A. et al. : Going with the flow : Hydrologic  
634 response of middle Lena River (Siberia) to the climate variability and change, *J. Hydrol.* 557, 475

635 - 488, <https://doi.org/10.1016/j.jhydrol.2017.12.034>, 2018.

636 Gebhardt, A. C., Gaye-Haake, B., Unger, D., Lahajnar, N., and Ittekkot, V.: A contemporary sediment  
637 and organic carbon budget for the Kara Sea shelf (Siberia), *Marine Geology* 220(1-4), 83-100,  
638 <https://doi.org/10.1016/j.margeo.2005.06.035>, 2005.

639 Gelfan, A., Gustafsson, D., Motovilov, Y., Arheimer, B., Kalugin, A., Krylenko, I., and Lavrenov A.:  
640 Climate change impact on the water regime of two great Arctic rivers: modelling and uncertainty  
641 issues, *Climate Change* 414(3), 499-515, DOI: 10.1007/s10584-016-1710-5m, 2017.

642 Georgiadi, A. G., Tananaev, N. I., and Dukhova L.A.: Hydrochemical conditions at the Lena River in  
643 August 2018, *Oceanology* 59(5), 797-800, <https://doi.org/10.1134/S0001437019050072>, 2019.

644 Goncalves-Araujo, R., Stedmon, C. A., Heim, B., Dubinenkov, I., Kraberg, A., Moiseev, D., and Brachler  
645 A.: From fresh to marine waters: Characterization and fate of dissolved organic matter in the Lena  
646 River delta region, Siberia, *Front. Marine Sci.*, 2, Art No 108,  
647 <https://doi.org/10.3389/fmars.2015.00108>, 2015.

648 Gordeev, V. V. and Sidorov, I. S.: Concentrations of major elements and their outflow into the Laptev  
649 Sea by the Lena River, *Mar. Chem.*, 43, 33–46, 1993.

650 Griffin, C. G., McClelland, J. W., Frey, K. E., Fiske, G., and Holmes, R. M.: Quantifying CDOM and  
651 DOC in major Arctic rivers during ice-free conditions using Landsat TM and ETM+ data. *Remote*  
652 *Sens. Environ.* 209, 395-409, doi: 10.1016/j.rse.2018.02.060, 2018.

653 Guérin, F., Abril, G., Serça, D., Delon, C., Richard, S., Delmas, R., Tremblay, A., and Varfalvy, L.: Gas  
654 transfer velocities of CO<sub>2</sub> and CH<sub>4</sub> in a tropical reservoir and its river downstream, *J. Mar. Syst.*,  
655 66, 161–172. <https://doi.org/10.1016/j.jmarsys.2006.03.019>, 2007.

656 Gureyev, D.: Tomsk State University: The expedition on the Lena River from the headwaters to the  
657 Aldan River, 2016. <https://www.youtube.com/watch?v=7IEiO4bgxc8>, 2016.

658 Harris, I., Jones, P. D., Osborn, T. J., and Lister, D. H.: Updated high-resolution grids of monthly climatic  
659 observations – the CRU TS3.10 Dataset, *Int. J. Climatol.*, 34: 623–642, doi: 10.1002/joc.3711,  
660 2014.

661 Hirst, K., Andersson, P., Kooijman, E., Kutscher, L., Maximov, T., Moth, C.-M., Porcelli, D.: Iron isotopes  
662 reveal the sources of Fe-bearing particles and colloids in the Lena River basin, *Geochim. Cosmochim.*  
663 *Acta*, 269, 678-692, doi: 10.1016/j.gca.2019.11.004, 2020.

664 Holmes, R.M., Coe, M.T., Fiske, G.J., Gurtovaya, T., McClelland, J.W., Shiklomanov, A.I., Spencer,  
665 R.G.M., Tank, S.E., and Zhulidov, A.V.: Climate change impacts on the hydrology and  
666 biogeochemistry of Arctic Rivers, In: *Climatic Changes and Global warming of Inland Waters: Impacts and Mitigation for Ecosystems and Societies*, Eds. C.R. Goldman, M. Kumagi, and R.D. Robarts, John Wiley and Sons, p. 1-26, 2013.

669 Horan, K.; Hilton, R. G., Dellinger, M., Tipper, E., Galy, V., Calmels, D., Selby, D., Gaillardet, J., Ottley,  
670 C.J., Parsons, D.R., and Burton, K.W.: Carbon dioxide emissions by rock organic carbon oxidation  
671 and the net geochemical carbon budget of the Mackenzie River Basin, *American J. Sci.* 319 (6) 473-  
672 499, DOI: <https://doi.org/10.2475/06.2019.02>, 2019.

673 Hotchkiss, E., Hall Jr, R., Sponseller, R. et al.: Sources of and processes controlling CO<sub>2</sub> emissions change  
674 with the size of streams and rivers, *Nature Geoscience*, 8, 696–699, <https://doi.org/10.1038/ngeo2507>,  
675 2015.

676 Hugelius, G., Tarnocai, C., Broll, G., Canadell, J. G., Kuhry, P., and Swanson, D. K.: The Northern  
677 Circumpolar Soil Carbon Database: spatially distributed datasets of soil coverage and soil carbon  
678 storage in the northern permafrost regions, *Earth Syst. Sci. Data*, 5, 3–13, <https://doi.org/10.5194/essd-5-3-2013>, 2013.

680 Huh, Y., Tsoi, M. Y., Zaitsev, A., and Edmond, J. M.: The fluvial geochemistry of the rivers of eastern  
681 Siberia: I. Tributaries of the Lena River draining the sedimentary platform of the Siberian Craton,  
682 *Geochim. Cosmochim. Acta*, 62, 1657-1676, doi: 10.1016/S0016-7037(98)00107-0, 1998a.

683 Huh, Y., Panteleyev, G., Babich, O., Zaitsev, A., and Edmond, J. M.: The fluvial geochemistry of the rivers  
684 of Eastern Siberia: II. Tributaries of the Lena, Omoloy, Yana, Indigirka, Kolyma, and Anadyr draining  
685 the collisional/accretionary zone of the Verkhoyansk and Cherskiy ranges, *Geochim. Cosmochim.*  
686 *Acta*, 62, 5063-5075, 1998b.

- 687 Huh, Y., and Edmond, J. M.: The fluvial geochemistry of the rivers of Eastern Siberia: III. Tributaries of the  
688 Lena and Anabar draining the basement terrain of the Siberian Craton and the Trans-Baikal Highlands,  
689 *Geochim. Cosmochim. Acta*, 63, 967–987, doi:10.1016/S0016-7037(99)00045-9, 1999.
- 690 Humborg, C., Morth, C.-M., Sundbom, M., Borg, H., Blenckner, T., Giesler, R., and Ittekkot, V.: CO<sub>2</sub>  
691 supersaturation along the aquatic conduit in Swedish watersheds as constrained by terrestrial  
692 respiration, aquatic respiration and weathering, *Glob. Change Biol.*, 16, 1966–1978,  
693 doi:10.1111/j.1365-2486.2009.02092.x, 2010.
- 694 Ivakhov, V. M., Paramonova, N. N., Privalov, V. I., Zinchenko, A. V., Loskutova, M. A., Makshtas, A.  
695 P., Kustov, V. Y., Laurila, T., Aurela, M., and Asmi, E.: Atmospheric Concentration of Carbon  
696 Dioxide at Tiksi and Cape Baranov Stations in 2010–2017, *Russian Meteorol. Hydrol.*, 44(4), 291–  
697 299, DOI: 10.3103/S1068373919040095, 2019.
- 698 Jähne, B., Heinz, G., and Dietrich, W.: Measurement of the diffusion coefficients of sparingly soluble gases  
699 in water, *J. Geophys. Res. Oceans* 92, 10767–10776, <https://doi.org/10.1029/JC092iC10p10767>,  
700 1987.
- 701 Johnson, M. S., Billett, M. F., Dinsmore, K. J., Wallin, M., Dyson, K. E., and Jassal, R. S.: Direct and  
702 continuous measurement of dissolved carbon dioxide in freshwater aquatic systems-method and  
703 applications, *Ecohydrology* 3(1), 68-78, doi:10.1002/eco, 2009.
- 704 Juhls, B., Stedmon, C. A., Morgenstern, A., Meyer, H., Holemann, J., Heim, B., Povazhnyi, V., and  
705 Overduin P. P.: Identifying drivers of seasonality in Lena River biogeochemistry and dissolved  
706 organic matter fluxes, *Front. Environ. Sci.*, 8, Art No 53, <https://doi.org/10.3389/fenvs.2020.00053>,  
707 2020.
- 708 Karlsson, J., Serikova, S., Rocher-Ros, G., Denfeld, B., Vorobyev, S. N., and Pokrovsky, O. S.: Carbon  
709 emission from Western Siberian inland waters, *Nature Communication* 12, 825,  
710 <https://doi.org/10.1038/s41467-021-21054-1>, 2021.
- 711 Klaus, M. and Vachon, D.: Challenges of predicting gas transfer velocity from wind measurements  
712 over global lakes, *Aquatic Sciences* 82, Art No 53, doi:10.1007/s00027-020-00729-9, 2020.
- 713 Klaus, M., Seekell, D. A., Lidberg, W., and Karlsson, J.: Evaluations of climate and land management  
714 effects on lake carbon cycling need to account temporal variability in CO<sub>2</sub> concentration,  
715 *Global Biogeochemical Cycles*, 33, 243-265, doi:10.1029/2018gb005979, 2019.
- 716 Kruse, S., Gerdes, A., Kath, N. J., Epp, L. S., Stoof-Leichsenring, K. R., Pestryakova, L. A., and Herzs Schuh,  
717 U.: Dispersal distances and migration rates at the arctic treeline in Siberia – a genetic and simulation-  
718 based study, *Biogeosciences*, 16, 1211–1224, <https://doi.org/10.5194/bg-16-1211-2019>, 2019.
- 719 Kutscher, L., Mörth, C.-M., Porcelli, D., Hirst, C., Maximov, T. C., Petrov, R. E., and Andersson, P. S.:  
720 Spatial variation in concentration and sources of organic carbon in the Lena River, Siberia, *J. Geophys.*  
721 *Res. Biogeosciences*, 122, 1999-2014, <https://doi.org/10.1002/2017JG003858>, 2017.
- 722 Kutzbach, L., Wille, C., and Pfeiffer, E.-M.: The exchange of carbon dioxide between wet arctic tundra and  
723 the atmosphere at the Lena River Delta, Northern Siberia, *Biogeosciences* 4(5), 869-890,  
724 <https://doi.org/10.5194/bg-4-869-2007>, 2007.
- 725 Kuzmin, M. I., Tarasova, E. N., Bychinskii, V. A., Karabanov, E. B., Mamontov, A. A., and Mamontova,  
726 E. A.: Hydrochemical regime components of Lena water, *Water Resources* 36(4), 418-430,  
727 <https://doi.org/10.1134/S0097807809040058>, 2009.
- 728 Lara, R. J., Rachold, V., Kattner, G., Hubberten, H. W., Guggenberger, G., Annelie, S., and Thomas, D. N.:  
729 Dissolved organic matter and nutrients in the Lena River, Siberian Arctic: Characteristics and  
730 distribution, *Marine Chemistry* 59, 301-309, doi: 10.1016/S0304-4203(97)00076-5, 1998.
- 731 Laurion, I., Massicotte, P., Mazoyer, F., Negandhi, K., and Mladenov, N.: Weak mineralization despite  
732 strong processing of dissolved organic matter in Eastern Arctic tundra ponds, *Limnol. Oceanogr.*, 66,  
733 (S1), S47-S63, doi: 10.1002/lno.11634, 2021.
- 734 Leith, F. I., Garnett, M. H., Dinsmore, K. J., Billett, M. F., and Heal, K. V.: Source and age of dissolved and  
735 gaseous carbon in a peatland-riparian-stream continuum: a dual isotope (<sup>14</sup>C and <sup>δ</sup><sup>13</sup>C) analysis,  
736 *Biogeochemistry*, 119, 415–433, doi:10.1007/s10533-014-9977-y, 2014.
- 737 Leith, F. I., Dinsmore, K. J., Wallin, M. B., Billett, M; F., Heal, K. V., Laudon, H., Öquist, M. G., and  
738 Bishop, K.: Carbon dioxide transport across the hillslope–riparian–stream continuum in a boreal  
739 headwater catchment, *Biogeosciences*, 12, 1–12, doi:10.5194/bg-12-1-2015, 2015.

740 Lobbes, J. M., Friznar, H. P., and Kattner, G.: Biogeochemical characteristics of the dissolved and particulate  
741 organic matter in Russian rivers entering the Arctic Ocean, *Geochim. Cosmochim. Acta*, 64(17),  
742 2973–2983, 2000.

743 McClelland, J. W., Holmes, R. M., Peterson, B. J., and Strieglitz, M.: Increasing river discharge in the  
744 Eurasian Arctic: Consideration of dams, permafrost thaw, and fires as potential agents of change, *J.*  
745 *Geophys. Res. Atmospheres*, 109 (D18), Art No D18102, doi:10.1029/2004JD004583, 2004.

746 McClelland, J. W., Déry, S. J., Peterson, B. J., Holmes, R. M., and Wood, E. F.: A pan-Arctic evaluation of  
747 changes in river discharge during the latter half of the 20<sup>th</sup> century, *Geophys. Res. Lett.*, 33, L06715,  
748 <https://doi.org/10.1029/2006GL025753>, 2006.

749 Murphy, M., Porcelli, D., Pogge von Strandmann, P., Hirst, K., Kutscher, L., Katchinoff, J., Morth, C.-  
750 M., Maximov, T., and Andresson, P.: Tracing silicate weathering processes in the permafrost-  
751 dominated Lena River watershed using lithium isotopes, *Geochim. Cosmochim. Acta*, 245, 154-  
752 171, doi:10.1016/j.gca.2018.10.024, 2018.

753 Park, J. H., Jin, H., Yoon, T. K., Begum, M. S., Eliyan, C., Lee, E.-J., Lee, S.-C., and Oh, N.-H.:  
754 Wastewater-boosted biodegradation amplifying seasonal variations of pCO<sub>2</sub> in the Mekong–Tonle  
755 Sap river system, *Biogeochemistry*, <https://doi.org/10.1007/s10533-021-00823-6>, 2021.

756 Park, J.-H., Nayna, O.K., Begum, M.S., Chea, E., Hartmann, J., Keil, R.G., Kumar, S., Lu, X., Ran, L.,  
757 Richey, J.E., Sarma, V.V.S.S, Tareq, S.M., Xuan, D. T., and Yu, R.: Reviews and syntheses:  
758 Anthropogenic perturbations to carbon fluxes in Asian river systems—concepts, emerging trends,  
759 and research challenges, *Biogeosciences* 15, 3049–3069. [https://doi.org/10.5194/bg-15-3049-](https://doi.org/10.5194/bg-15-3049-2018)  
760 2018, 2018.

761 Payandi-Rolland, D., Shirokova, L. S., Nakhle, P., Tesfa, M., Abdou, A., Causserand, C., Lartiges, B.,  
762 Rols, J.L., Guérin, F., Bénézech, P., and Pokrovsky, O.S.: Aerobic release and biodegradation of  
763 dissolved organic matter from frozen peat: Effects of temperature and heterotrophic bacteria,  
764 *Chem. Geol.* 536, Art No 119448, <https://doi.org/10.1016/j.chemgeo.2019.119448>, 2020.

765 Pekel, J. F., Cottam, A., Gorelick, N. et al.: High-resolution mapping of global surface water and its long-  
766 term changes, *Nature*, 540, 418–422, <https://doi.org/10.1038/nature20584>, 2016.

767 Pipko, I. I., Pugach, S. P., Savichev, O. G., Repina, I. A., Shakhova, N. E., Moiseeva, Yu. A., Barskov, K.  
768 V., Sergienko, V. I., and Semiletov, I. P.: Dynamics of dissolved inorganic carbon and CO<sub>2</sub> fluxes  
769 between the water and the atmosphere in the main channel of the Ob River, *Doklady Chemistry*  
770 484(2), 52-57, doi:10.1134/S0012500819020101, 2019.

771 Pipko; I. I., Pugach, S. P., Dudarev, O. V., Charkin, A. N., and Semiletov, I. P.: Carbonate parameters  
772 of the Lena River: Characteristics and distribution, *Geochem. Internat.*, 48(11), 1131-1137,  
773 <https://doi.org/10.1134/S0016702910110078>, 2010.

774 Qin, J., Huh, Y., Edmond, J. M., Du, G., and Ran, J.: Chemical and physical weathering in the Min  
775 Jiang, a headwater tributary of the Yangtze River, *Chem. Geol.*, 227, 53–69,  
776 doi:10.1016/j.chemgeo.2005.09.011, 2006.

777 Rachold, V., Alabyan, A., Hubberten, H.-W., Korotaev, V. N., and Zaitsev, A. A.: Sediment transport  
778 to the Laptev Sea - hydrology and geochemistry of the Lena River, *Polar Research*, 15(2), 183-  
779 196, doi: <https://doi.org/10.3402/polar.v15i2.6646>, 1996.

780 Raymond, P. A., McClelland, J. W., Holmes, R. M., Zhulidov, A. V., Mull, K. et al.: Flux and age of  
781 dissolved organic carbon exported to the Arctic Ocean: A carbon isotopic study of the five  
782 largest arctic rivers, *Global Biogeochemical Cycles*, 121, Art No GB4011,  
783 <https://doi.org/10.1029/2007GB002934>, 2007.

784 Raymond, P. A., Hartmann, J., Lauerwald, R., Sobek, S., McDonald, C., Hoover, M., Butman, D., Striegl,  
785 R., Mayorga, E., Humborg, C., Kortelainen, P., Dürr, H., Meybeck, M., Ciais, P., and Guth, P.:  
786 Global carbon dioxide emissions from inland waters, *Nature*, 503, 355–359,  
787 doi:10.1038/nature12760, 2013.

788 Rocher-Ros, G., Sponseller, R. A., Lidberg, W., Mörth, C-M., and Giesler, R.: Landscape process  
789 domains drive patterns of CO<sub>2</sub> evasion from river networks, *Limnol. Oceanogr. Lett.*, 4, 87-95,  
790 <https://doi.org/10.1002/lol2.10108>, 2019.

791 Sachs, T., Wille, C., Boike, J., and Kutzbach, L.: Environmental controls on ecosystem-scale CH<sub>4</sub> emission  
792 from polygonal tundra in the Lena River Delta, Siberia, *J. Geophys. Research Biogeosciences*, 113,  
793 Art No G00A03, <https://doi.org/10.1029/2007JG000505>, 2008.

794 Santoro, M., Beer, C., Cartus, O., Schmullius, C., Shvidenko, A., McCallum, I., Wegmueller, U., and  
795 Wiesmann, A.: The BIOMASAR algorithm: An approach for retrieval of forest growing stock volume  
796 using stacks of multi-temporal SAR data, In: *Proceedings of ESA Living Planet Symposium*, 28 June-  
797 2 July 2010 (<https://www.researchgate.net/publication/230662433>,  
798 <http://pure.iiasa.ac.at/id/eprint/9430/>), 2010.

799 Schuur, E. A. G., McGuire, A. D., Schädel, C., Grosse, G., Harden, J. W., Hayes, D. J., Hugelius, G., Koven,  
800 C. D., Kuhry, P., Lawrence, D. M., Natali, S. M., Olefeldt, C., Romanovsky, V. E., Schaefer, K.,  
801 Turetsky, M. R., Treat, C. C., and Vonk, J. E.: Climate change and the permafrost carbon feedback,  
802 *Nature* 520, 171–179, <http://dx.doi.org/10.1038/nature14338>, 2015.

803 Semiletov, I. P.: Aquatic sources and sinks of CO<sub>2</sub> and CH<sub>4</sub> in the polar regions, *J. Atmospheric Sci.*, 56,  
804 286-306, [https://doi.org/10.1175/1520-0469\(1999\)056<0286:ASASOC>2.0.CO;2](https://doi.org/10.1175/1520-0469(1999)056<0286:ASASOC>2.0.CO;2), 1999.

805 Semiletov, I. P., Pipko, I. I., Shakhova, N. E., Dudarev, O. V., Pugach, S. P., Charkin, A. N., McRoy, C. P.,  
806 Kosmach, D., Gustafsson Ö.: Carbon transport by the Lena River from its headwaters to the Arctic  
807 Ocean, with emphasis on fluvial input of terrestrial particulate organic carbon vs. carbon transport by  
808 coastal erosion, *Biogeosciences*, 8, 2407–2426, <https://doi.org/10.5194/bg-8-2407-2011>, 2011.

809 Serikova, S., Pokrovsky, O. S., Ala-aho, P., Kazantsev, V., Kirpotin, S. N., Kopysov, S. G., Krickov, I. V.,  
810 Laudon, H., Manasypov, R. M., Shirokova, L. S., Sousby, C., Tetzlaff, D., and Karlsson, J.: High  
811 riverine CO<sub>2</sub> emissions at the permafrost boundary of Western Siberia, *Nat. Geosci.*, 11, 825–829,  
812 <https://doi.org/10.1038/s41561-018-0218-1>, 2018.

813 Serikova S., Pokrovsky O. S., Laudon, H., Krickov, I. V., Lim, A. G., Manasypov, R. M., and Karlsson, J.:  
814 C emissions from lakes across permafrost gradient of Western Siberia, *Nat. Commun.*, 10, 1552,  
815 <https://doi.org/10.1038/s41467-019-09592-1>, 2019.

816 Siewert, M. B., Hugelius, G., Heim, B., and Faucherre, S.: Landscape controls and vertical variability of soil  
817 organic carbon storage in permafrost-affected soils of the Lena River Delta, *Catena*, 147, 725-741,  
818 doi:10.1016/j.catena.2016.07.048, 2016.

819 Smith, L. C., Pavelksky, T. M.: Estimation of river discharge, propagation speed, and hydraulic  
820 geometry from space: Lena River, Siberia, *Water Resources Res.*, 44(3), W03427,  
821 <https://doi.org/10.1029/2007WR006133>, 2008.

822 Spence, J. and Telmer, K.: The role of sulfur in chemical weathering and atmospheric CO<sub>2</sub> fluxes:  
823 evidence from major ions,  $\delta^{13}\text{C}_{\text{DIC}}$ , and  $\delta^{34}\text{S}_{\text{SO}_4}$  in rivers of the Canadian Cordillera, *Geochim.*  
824 *Cosmochim. Acta*, 69, 5441–5458, doi:10.1016/j.gca.2005.07.011, 2005.

825 Stackpoole, S. M., Butman, D. E., Clow, D. W., Verdin, K. L., Gaglioti, B. V., Genet, H., and Striegl,  
826 R. G.: Inland waters and their role in the carbon cycle of Alaska, *Ecological Applications* 27(5),  
827 1403-1420, doi:10.1002/eap.1552/full, 2017.

828 Striegl, R. G., Dornblaser, M. M., McDonald, C. P., Rover, J. R., and Stets E. G.: Carbon dioxide and  
829 methane emissions from the Yukon River system, *Global Biogeochem. Cycles*, 26, GB0E05,  
830 doi:10.1029/2012GB004306, 2012.

831 Sun X., Mörth C.-M., Porcelli D., Kutscher L., Hirst C., Murphy M. J., Maximov T., Petrov R. E.,  
832 Humborg C., Schmitt M. and Andersson P. S.: Stable silicon isotopic compositions of the Lena  
833 River and its tributaries: Implications for silicon delivery to the Arctic Ocean, *Geochim.*  
834 *Cosmochim. Acta* 241, 120–133, doi: 10.1016/j.gca.2018.08.044, 2018.

835 Suzuki, K., Matsuo, K., Yamazaki, D., Ichii, K., Iijima, Y., Papa, F., Yanagi, Y., and Hiyama, T.:  
836 Hydrological variability and changes in the Arctic circumpolar tundra and the three largest Pan-  
837 Arctic river basins from 2002 to 2016, *Remote Sensing* 10, Art No 402, doi:10.3390/rs10030402,  
838 2018.

839 Vachon, D., Prairie, Y. T., and Cole, J. J.: The relationship between near-surface turbulence and gas  
840 transfer velocity in freshwater systems and its implications for floating chamber measurements of  
841 gas exchange, *Limnology and Oceanography*, 55(4), 1723–173, doi:10.4319/lo.2010.55.4.1723,  
842 2010.

- 843 Van der Molen, M. K., van Huissteden J., Parmentier F. J. W., Petrescu, A. M. R., Dolman, A. J.,  
844 Maximov, T. C. et al.: The growing season greenhouse gas balance of a continental tundra site in  
845 the Indigirka lowlands, NE Siberia, *Biogeosciences* 4(6), 985-1003, [https://doi.org/10.5194/bg-4-](https://doi.org/10.5194/bg-4-985-2007)  
846 [985-2007](https://doi.org/10.5194/bg-4-985-2007), 2007.
- 847 Vonk, J. E., Tank, S. E., Mann, P. J., Spencer, R. G. M., Treat, C. C., Striegl, R. G., Abbott, B. W., and  
848 Wickland, K. P.: Biodegradability of dissolved organic carbon in permafrost soils and aquatic  
849 systems: a meta-analysis, *Biogeosciences*, 12, 6915–6930, [https://doi.org/10.5194/bg-12-6915-](https://doi.org/10.5194/bg-12-6915-2015)  
850 [2015](https://doi.org/10.5194/bg-12-6915-2015), 2015.
- 851 Vonk, J. E., Tank, S. E., and Walvoord, M. A.: Integrating hydrology and biogeochemistry across frozen  
852 landscapes, *Nat. Commun.* 10, 1–4. <https://doi.org/10.1038/s41467-019-13361-5>, 2019.
- 853 Wanninkhof, R.: Relationship between wind speed and gas exchange over the ocean, *J. Geophys. Res.*  
854 *97*, 7373–7382, <https://doi.org/10.4319/lom.2014.12.351>, 1992.
- 855 Ward, C. P., Nalven, S. G., Crump, B. C., Kling, G. W., and Cory, R. M.: Photochemical alteration of  
856 organic carbon draining permafrost soils shifts microbial metabolic pathways and stimulates  
857 respiration, *Nat. Commun.*, 8, 772, <https://doi.org/10.1038/s41467-017-00759-2>, 2017.
- 858 Wild, B., Andersson, A., Bröder, L., Vonk, J., Hugelius, G., McClelland, J. W., Song, W., Raymond P.  
859 A., and Gustafsson, Ö.: Rivers across the Siberian Arctic unearth the patterns of carbon release  
860 from the thawing permafrost, *PNAS* 116(21), 10280-10285,  
861 <https://doi.org/10.1073/pnas.1811797116>, 2019.
- 862 Wille, C., Kutzbach, L., Sachs, T., Wagner, D., and Pfeiffer, E.M.: Methane emission from Siberian  
863 arctic polygonal tundra: eddy covariance measurements and modeling, *Global Change Biology*  
864 *14*(6), 1395-1408, <https://doi.org/10.1111/j.1365-2486.2008.01586.x>, 2008.
- 865 Wu, L. and Huh, Y.: Dissolved reactive phosphorus in large rivers of East Asia, *Biogeochemistry* 85,  
866 263-288, doi:10.1007/s10533-007-9133-z, 2007.
- 867 Yang, D. Q., Kane, D. L., Hinzman, L. D., Zhang, X. B., Zhing, T. J., and Ye, H. C.: Siberian Lena River  
868 hydrological regime and recent change, *J. Geophys. Res. Atmospheres* 107, D23, Art No 4694,  
869 <https://doi.org/10.1029/2002JD002542>, 2002.
- 870 Yamamoto, S., Alcauskas, J. B., and Crozier, T.E.: Solubility of methane in distilled water and seawater,  
871 *J. Chem. Eng. Data*, 21(1), 78– 80, doi:10.1021/je60068a029, 1976.
- 872 Ye, B., Yang, D., Zhang, Z., and Kane, D. L.: Variation of hydrological regime with permafrost coverage  
873 over Lena basin in Siberia, *J. Geophys. Res.*, 114, D07102, doi:10.1029/2008JD010537, 2009.
- 874 Yoon, T. K., Jin, H., Oh, N.-H., and Park, J.-H.: Technical note: Assessing gas equilibration systems for  
875 continuous pCO<sub>2</sub> measurements in inland waters, *Biogeosciences*, 13, 3915–3930,  
876 <https://doi.org/10.5194/bg-13-3915-2016>, 2016.
- 877 Zhang, T., Frauenfeld, O. W., Serreze, M. C., Etringer, A., Oelke, C. et al.: Spatial and temporal  
878 variability in active layer thickness over the Russian Arctic drainage basin, *J. Geophys. Res.*, 110,  
879 D16101, doi: 10.1029/2004JD005642, 2005.
- 880 Zubrzycki, S., Kutzbach, L., Grosse, G., Desyatkin, A., and Pfeiffer, E. M.: Organic carbon and total  
881 nitrogen stocks in soils of the Lena River Delta, *Biogeosciences* 10, 3507-3524, doi:10.5194/bg-
- 882 [10-3507-2013](https://doi.org/10.5194/bg-10-3507-2013), 2013.

883  
884  
885  
886  
887  
888  
889

890 **Table 1.** Measured water temperature, pCO<sub>2</sub>, calculated CO<sub>2</sub> flux, CH<sub>4</sub>, DOC, and DIC concentrations  
 891 and pH in the Lena River main stem (average ± s.d.; (n) is number of measurements).

892

River transect	T <sub>water</sub> , °C	pCO <sub>2</sub> , µatm	FCO <sub>2</sub> , g C m <sup>-2</sup> d <sup>-1</sup> k = 4.464
Lena upstream of Kirenga (0-578 km)	12.65±0.22 (99)	714±22 (99)	0.849±0.061 (99)
Lena Kirenga – Vitim (579-1132 km)	9.17±0.15 (87)	806±8.8 (87)	1.19±0.024 (87)
Lena Vitim -Nuya (1132-1331 km)	8.10±0.115 (27)	797±22 (27)	1.22±0.072 (27)
Lena Nuya – Tuolba (1331-2008 km)	9.61±0.09 (95)	846±12 (95)	1.29±0.034 (95)
Lena Tuolba – Aldan (2008-2381 km)	10.6±0.21 (52)	1003±28 (52)	1.69±0.081 (5)

893

	CH <sub>4</sub> , µmol L <sup>-1</sup>	DOC, mg L <sup>-1</sup>	DIC, mg L <sup>-1</sup>	pH
Lena upstream of Kirenga (0-578 km)	0.068±0.003 (6)	13.9±1.4 (6)	20.0±1.2 (6)	8.12±0.203 (7)
Lena Kirenga – Vitim (579-1132 km)	0.040±0.002 (12)	7.55±0.246 (14)	6.30±0.485 (14)	7.77±0.040 (14)
Lena Vitim -Nuya (1132-1331 km)	0.038±0.003 (5)	9.02±0.29 (3)	4.55±0.70 (3)	7.69±0.063 (3)
Lena Nuya – Tuolba (1331-2008 km)	0.037±0.002 (6)	10.4±0.78 (2)	5.09±1.157 (2)	7.62±0.052 (2)
Lena Tuolba – Aldan (2008-2381 km)	0.088±0.034 (5)	11.6±0.27 (5)	5.24±0.102 (5)	7.49±0.044 (5)

894

895

896

897

898

899

900

901

902

903

904

905

906

907

908

909

910

911

912

913

914

915

916

917 **Table 2.** Measured water temperature, pCO<sub>2</sub>, calculated CO<sub>2</sub> flux, CH<sub>4</sub>, DOC, DIC concentration and  
 918 pH in the tributaries (average ± s.d.; (n) is number of measurements).

919

Tributary	T <sub>water</sub> , °C	pCO <sub>2</sub> , µatm	FCO <sub>2</sub> , g C m <sup>-2</sup> d <sup>-1</sup>
<b>№4 Orlinga (208 km)</b>	8.0±0.0 (13)	515±2.9 (13)	0.347±0.01 (13)
<b>№5 Nijnaya Kitima (228 km)</b>	6.8±0.0 (11)	462±9.4 (11)	0.193±0.03 (11)
<b>№8 Taiur (416 km)</b>	8.5±0.0 (10)	575±31 (10)	0.523±0.095 (10)
<b>№10 Bol. Tira (529 km)</b>	11.9±0.0 (15)	788±12 (15)	1.04±0.03 (15)
<b>№12 Kirenga (579 km)</b>	10.2±0.0 (323)	448±4 (323)	0.131±0.01 (323)
<b>№25 Thcayka (1025 km)</b>	8.6±0.01 (8)	856±13 (8)	1.37±0.04 (8)
<b>№28 Tchuya (1110 km)</b>	5.9±0.0 (5)	751±5.7 (5)	1.16±0.019 (5)
<b>№29 Vitim (1132 km)</b>	6.8±0.0 (10)	654±10 (10)	0.812±0.03 (10)
<b>№32 Ykte (1265 km)</b>	4.9±0.0 (11)	676±4.8 (11)	0.943±0.02 (11)
<b>№34 Kenek (1312 km)</b>	7.60±0.0 (11)	710±2.6 (11)	0.964±0.01 (11)
<b>№36 Nuya (1331 km)</b>	11.8±0.0 (10)	752±6.0 (10)	0.947±0.02 (10)
<b>№38 Bol. Patom (1670 km)</b>	6.9±0.0 (5)	730±12 (5)	1.05±0.04 (5)
<b>№39 Biriuk (1712 km)</b>	14.2±0.0 (5)	929±19 (5)	1.32±0.05 (5)
<b>№40 Olekma (1750 km)</b>	6.4±0.0 (11)	802±14 (11)	1.30±0.05 (11)
<b>№43 Markha (1948 km)</b>	17.5±0.0 (15)	844±15 (15)	0.998±0.03 (15)
<b>№44 Tuolba (2008 km)</b>	12.3±0.0 (305)	1181±6 (305)	2.08±0.02 (305)
<b>№46 Siniaya (2118 km)</b>	18.5±0.0 (24)	894±19 (24)	1.08±0.04 (24)
<b>№48 Buotama (2170 km)</b>	18.5±0.0 (24)	1160±25 (24)	1.66±0.06 (24)
<b>№52-54 Aldan (2381 km)</b>	14.8±0.02 (316)	1715±12 (316)	3.23±0.03 (316)

920

921

922

923

924

925

926

927

928

929

930

931

932

933

934 **Table 2**, continued.

935

	<b>CH<sub>4</sub>, μmol L<sup>-1</sup></b>	<b>DOC, mg L<sup>-1</sup></b>	<b>DIC, mg L<sup>-1</sup></b>	<b>pH</b>
<b>№4 Orlinga (208 km)</b>	0.064	13.4	27.9	8.64
<b>№5 Nijnaya Kitima (228 km)</b>	0.033	16.7	13.1	8.48
<b>№8 Taiur (416 km)</b>	0.079	10.0	11.2	8.36
<b>№10 Bol. Tira (529 km)</b>	0.084	22.7	14.9	8.13
<b>№12 Kirenga (579 km)</b>	0.036	5.13	6.86	7.97
<b>№25 Thcayka (1025 km)</b>	0.066	16.7	22.5	8.30
<b>№28 Tchuya (1110 km)</b>	0.037	7.08	3.44	7.57
<b>№29 Vitim (1132 km)</b>	0.057	10.1	2.18	7.70
<b>№32 Ykte (1265 km)</b>	0.037	5.49	15.3	7.86
<b>№34 Kenek (1312 km)</b>	0.053	21.1	16.0	8.12
<b>№36 Nuya (1331 km)</b>	0.048	26.6	11.7	7.80
<b>№38 Bol. Patom (1670 km)</b>	0.026	6.99	4.56	7.76
<b>№39 Biriuk (1712 km)</b>	0.047	29.2	11.3	7.87
<b>№40 Olekma (1750 km)</b>	0.046	13.3	3.3	7.53
<b>№43 Markha (1948 km)</b>	0.088	27.4	10.9	8.00
<b>№44 Tuolba (2008 km)</b>	0.035	14.5	14.7	7.98
<b>№46 Siniaya (2118 km)</b>	0.113	33.2	7.73	7.97
<b>№48 Buotama (2170 km)</b>	0.124	12.2	31.6	8.45
<b>№52-54 Aldan (2381 km)</b>	0.088 (4)	9.07±0.75 (4)	6.67±0.13 (4)	7.59±0.02 (4)

936

937 Footnote : in all tributaries except Aldan, there was only one measurement of CH<sub>4</sub>, DOC, DIC and pH

938

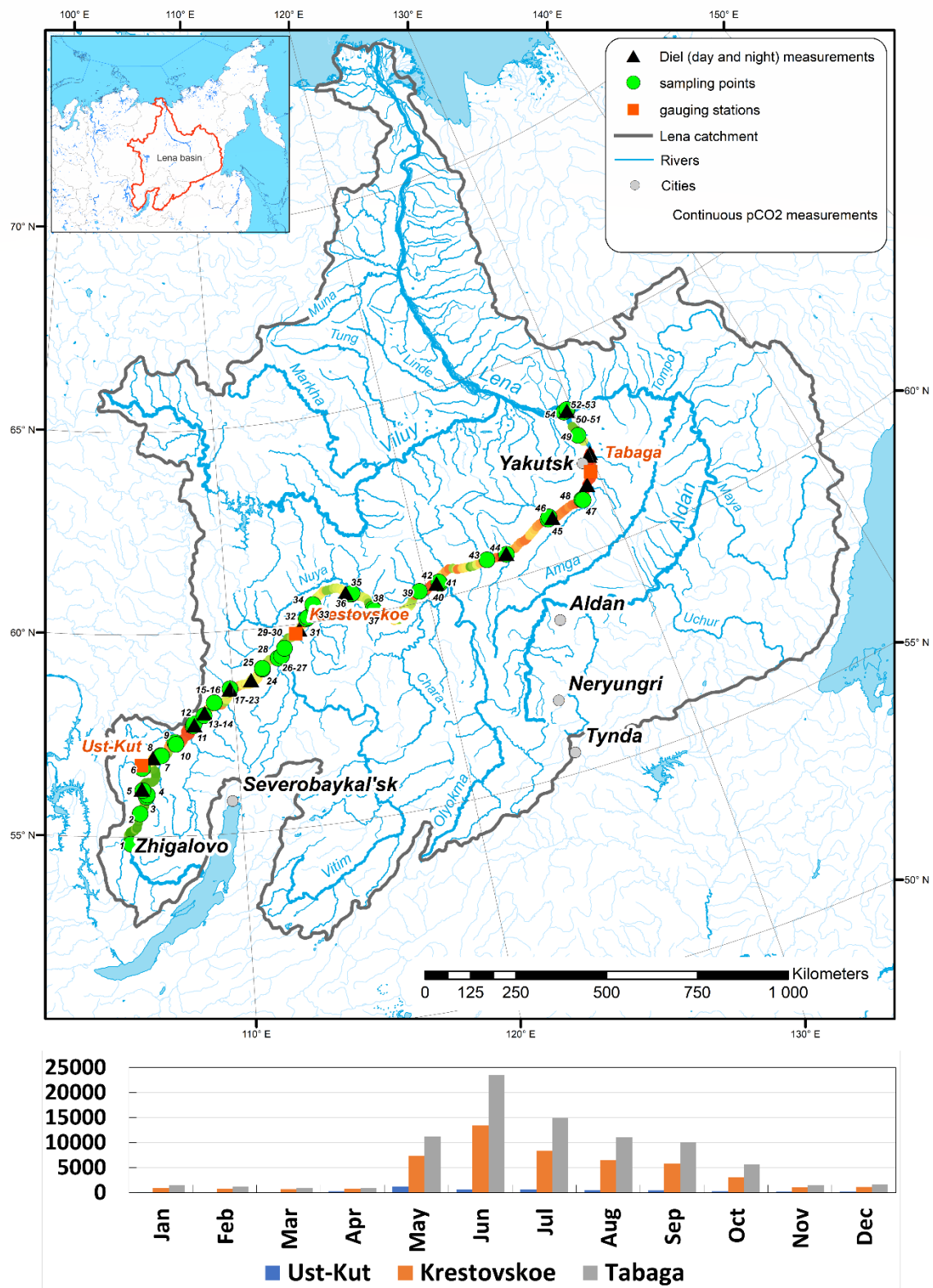
939 **Table 3.** Pearson correlations between pCO<sub>2</sub> and landscape parameters of the Lena tributaries.  
 940 Significant correlations ( $p < 0.05$ ) are marked by asterisk. Methane concentration did not exhibit any  
 941 significant correlation with all tested parameters.

942

% coverage of the watershed and climate	$R_{\text{Pearson}}$
Broadleaf Forest	0.04
Humid Grassland	-0.52*
Shrub Tundra	-0.05
Riparian Vegetation	0.87*
Croplands	-0.31
Bare Soil and Rock	0.54*
Evergreen Needle-leaf Forest	-0.59*
Deciduous Broadleaf Forest	-0.14
Mixed Forest	-0.34
Deciduous Needle-leaf Forest	0.56*
Bogs and marches	0.44
Palsa bogs	0.29
Recent burns	-0.25
Water bodies	0.63*
Aboveground biomass	-0.55*
Soil C stock, 0-30 cm	0.54*
Soil C stock, 0-100 cm	0.65*
Carbonate rocks	0.20
Continuous permafrost	0.66*
Discontinuous permafrost	-0.27
Sporadic permafrost	-0.43
Isolated permafrost	-0.19
Mean annual air temperature	-0.76*
Mean annual precipitation, mm	0.10

944

945

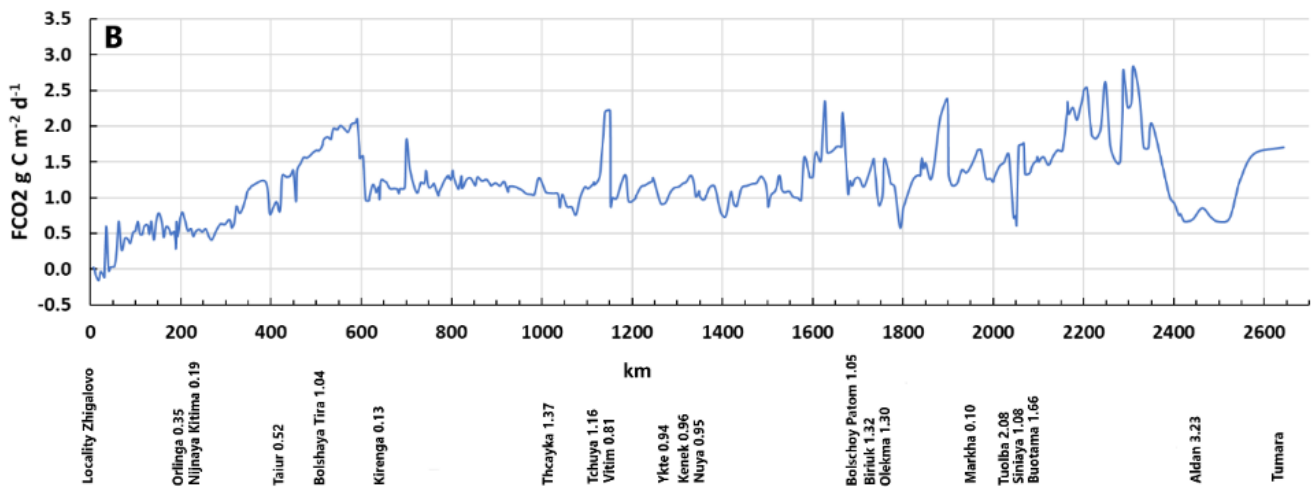
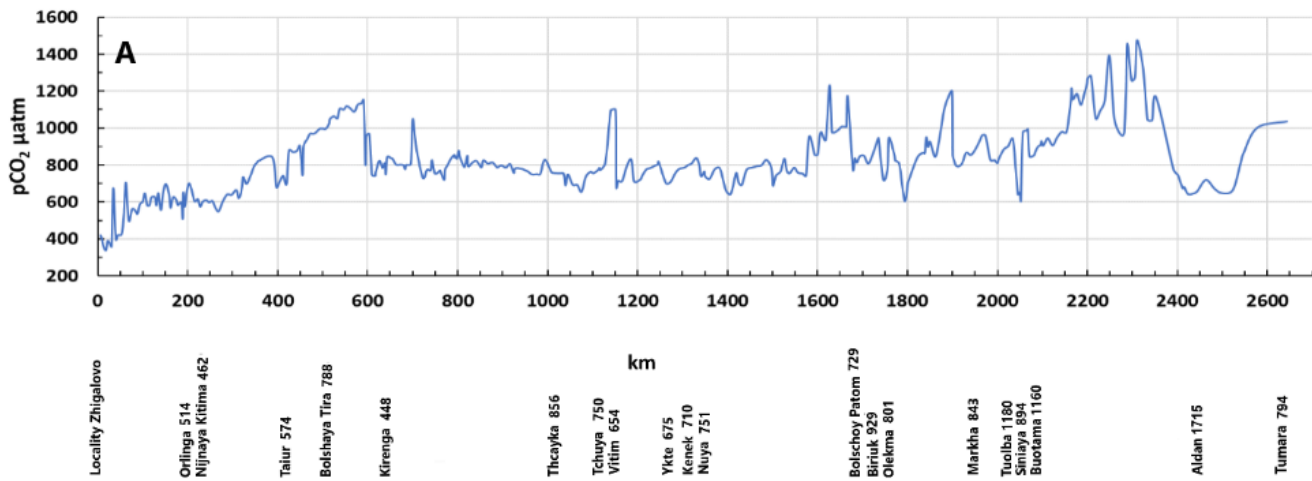


946

947 **Fig. 1.** Map of the studied Lena River watershed with continuous pCO<sub>2</sub> measurements in the main  
 948 stem. Mean multi-annual hydrographs of Ust-Kut, Krestovskoe and Tabaga station (labelled in red on  
 949 the map) are provided in the insert.

950

951



95:  
953  
954

95!  
956

957

958

959 **Figure 2.** A 20-km averaged pCO<sub>2</sub> profile (A) and calculated CO<sub>2</sub> fluxes (B) of the Lena River main  
 960 stem of over 2600 km distance, from Zhigalovo to the Tumara River. The average pCO<sub>2</sub> (μatm) and  
 961 fluxes (g C m<sup>-2</sup> d<sup>-1</sup>) of the main sampled tributaries are provided as numbers below X axes. Note that  
 962 peaks of CO<sub>2</sub> concentration at the main stem are not linked to conflux with tributaries.

963

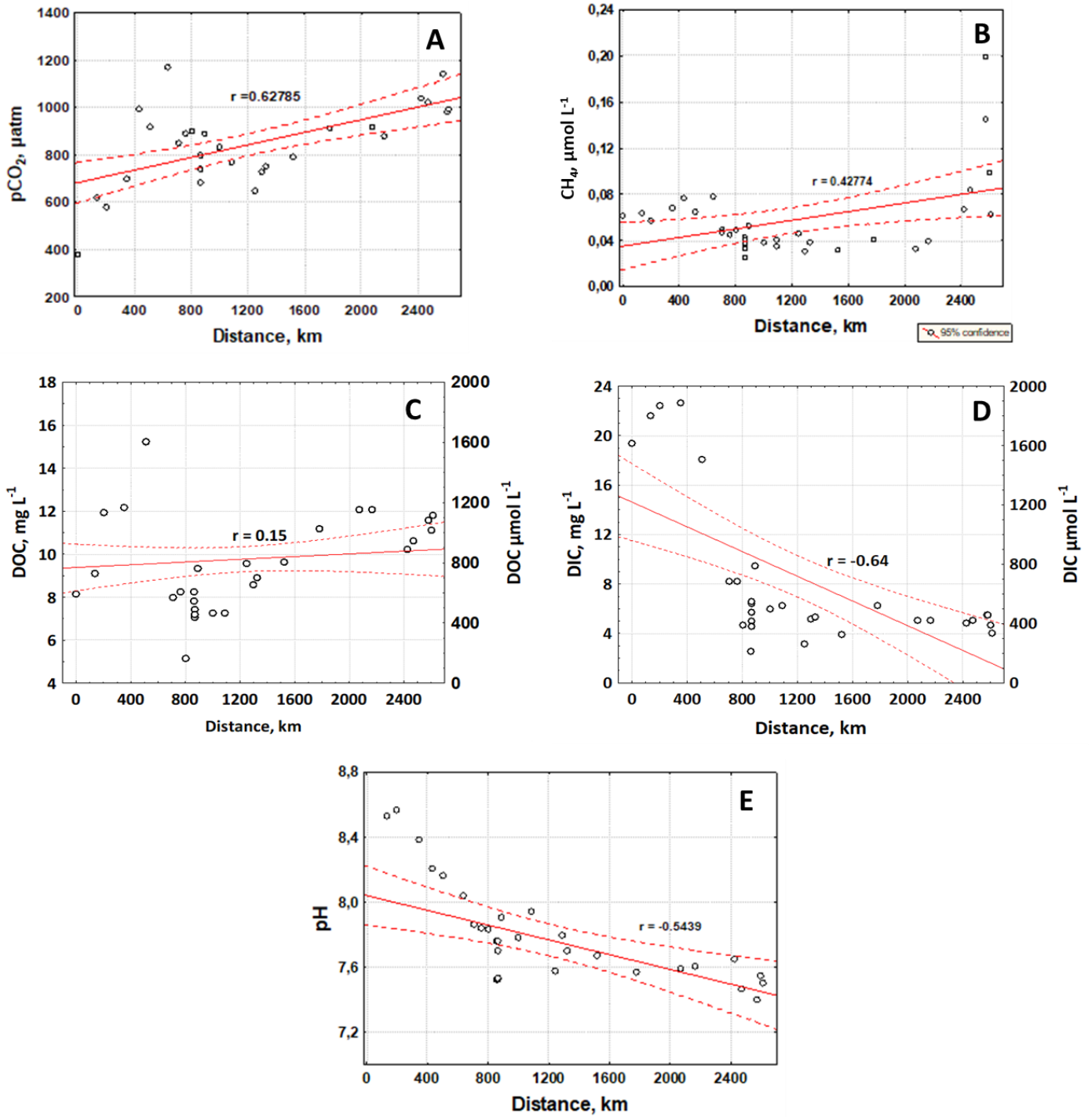
964

965

966

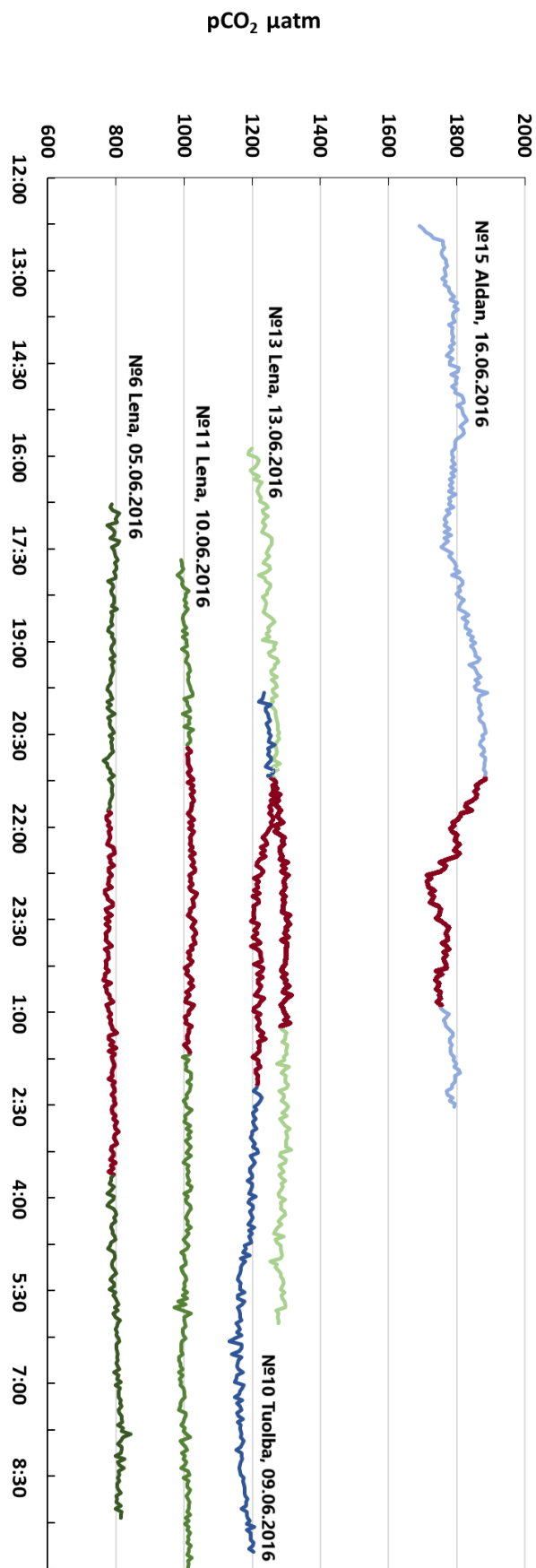
967

968



969  
 970  
 971  
 972  
 973  
 974  
 975  
 976

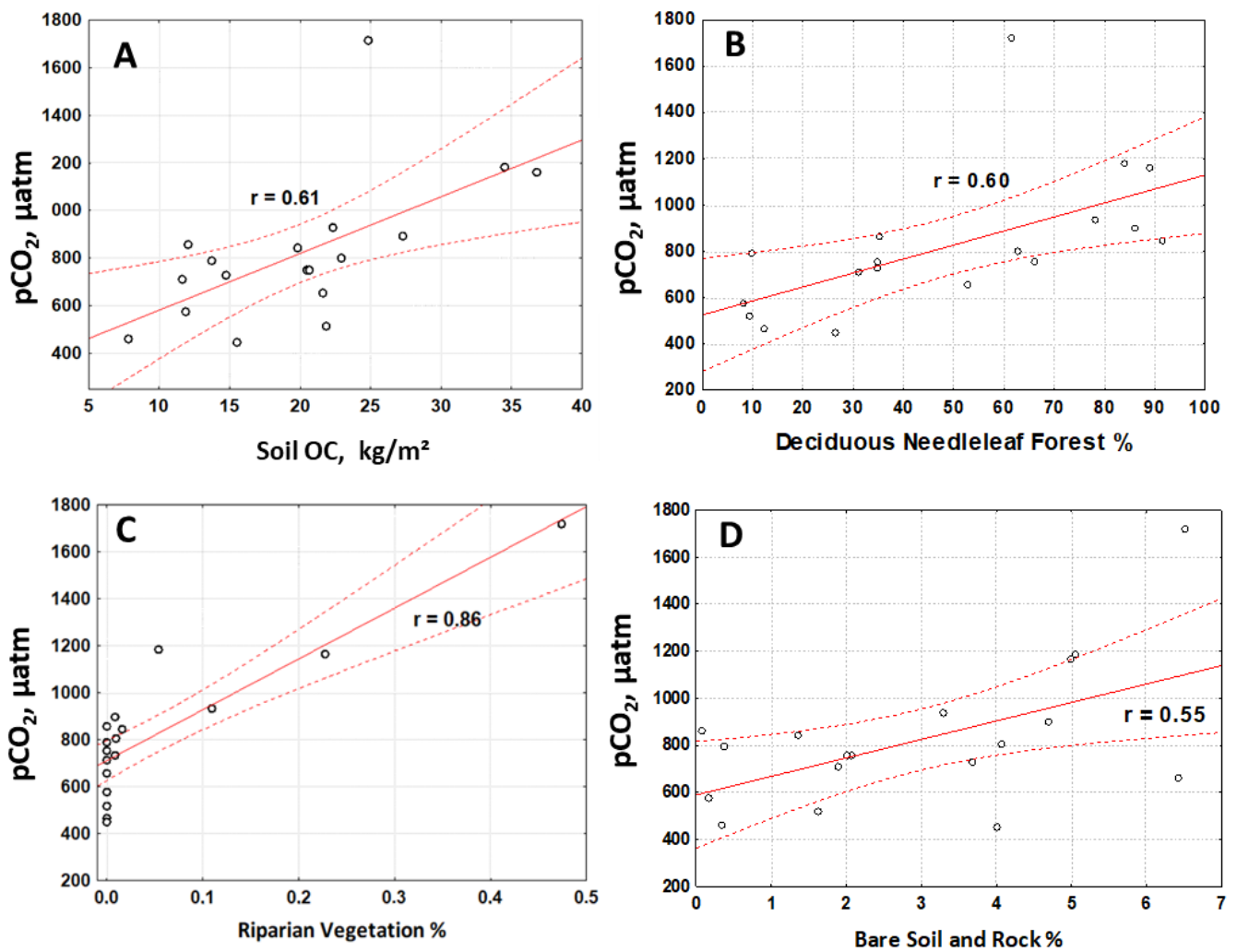
**Figure 3.** Averaged (over 20-km distance) CO<sub>2</sub> (A), CH<sub>4</sub> (B), DOC (C), DIC (D) and pH (E) concentration over the distance of the boat route at the Lena River, from the south-west to north-east.



977

978 **Figure 4.** Continuous pCO<sub>2</sub> concentration in the Lena River and two tributaries from late afternoon to  
 979 morning next day. Red part of the line represents night time. Variations of water temperature did not  
 980 exceed 2 °C.

981  
982  
983  
984  
985  
986  
987  
988  
989  
990



991  
992  
993

994 **Figure 5.** Significant ( $p < 0.05$ ) positive control of landscape parameters – OC stock in 0-100 cm of  
995 soil (A), and proportion of deciduous needle-leaf forest (B), riparian vegetation (C) and bare soil and  
996 rock (D) in the watershed on pCO<sub>2</sub> in the Lena River tributaries.